nature neuroscience

A microRNA switch regulates the rise in hypothalamic GnRH production before puberty

Andrea Messina[1,2,8], Fanny Langlet[1–3,9], Konstantina Chachlaki[1,2,9], Juan Roa[4–6,9], Sowmyalakshmi Rasika[7], Nathalie Jouy[1,2], Sarah Gallet[1,2], Francisco Gaytan[4–6], Jyoti Parkash[1,2,8], Manuel Tena-Sempere[4–6], Paolo Giacobini[1,2] & Vincent Prevot[1,2]

A sparse population of a few hundred primarily hypothalamic neurons forms the hub of a complex neuroglial network that controls reproduction in mammals by secreting the 'master molecule' gonadotropin-releasing hormone (GnRH). Timely postnatal changes in GnRH expression are essential for puberty and adult fertility. Here we report that a multilayered microRNA-operated switch with built-in feedback governs increased GnRH expression during the infantile-to-juvenile transition and that impairing microRNA synthesis in GnRH neurons leads to hypogonadotropic hypogonadism and infertility in mice. Two essential components of this switch, miR-200 and miR-155, respectively regulate *Zeb1*, a repressor of *Gnrh* transcriptional activators and *Gnrh* itself, and *Cebpb*, a nitric oxide–mediated repressor of *Gnrh* that acts both directly and through *Zeb1*, in GnRH neurons. This alteration in the delicate balance between inductive and repressive signals induces the normal GnRH-fuelled run-up to correct puberty initiation, and interfering with this process disrupts the neuroendocrine control of reproduction.

The onset of puberty and the regulation of fertility in mammals are governed by a complex, primarily hypothalamic neural network that converges onto GnRH-producing neurons, the master regulators of gonadotropin secretion and postnatal gonadal growth and function[1]. Proper GnRH system development[2], including timely changes in GnRH expression and signaling by this sparse population of a few hundred neurons[3,4], is essential for sexual maturation and the normal hypothalamic–pituitary–gonadal (HPG) axis functioning. However, despite the identification of several factors influencing GnRH production and release[1] the mechanisms regulating the clocklike precision of the pubertal activation process remain largely unknown.

MicroRNAs (miRNAs) are short (~22-nucleotide) noncoding RNAs that silence gene expression post-transcriptionally, principally by binding to 3′ untranslated regions (3′ UTR) of target mRNAs (**Supplementary Fig. 1**). Mature miRNAs are known to be required for the normal differentiation and function of several cell types[5] and, in particular, to regulate somatic growth and fertility at the level of peripheral organs[6,7]. We therefore asked whether miRNAs could play a similarly critical role in the central neuroendocrine control of reproduction.

Here we show that a switch in miRNA expression patterns in infantile GnRH neurons inverts the balance between inductive and repressive signals, triggering increased hypothalamic GnRH expression and controlling the crucial transition from the early infantile phase, when its levels are low, to the GnRH-fuelled run-up to puberty. These data raise the intriguing possibility that miRNA-dependent epigenetic regulation of GnRH secretion could underlie the pathophysiology of human hypogonadotropic hypogonadism when a genetic cause is not evident, and they hold therapeutic potential for puberty and infertility disorders of hypothalamic origin.

RESULTS

Dicer loss in GnRH neurons causes infertility

To determine whether miRNAs are involved in the crucial postnatal increase in GnRH expression, we generated mice in which Dicer, an RNAse-III endonuclease essential for miRNA biogenesis[8], was selectively inactivated in GnRH neurons. Mice harboring a *loxP*-flanked *Dicer* allele[5] were crossed with those expressing Cre recombinase under the control of the endogenous *Gnrh* promoter[9] (**Fig. 1a**), which drives expression in hypothalamic GnRH neurons but not the gonads (**Supplementary Fig. 2a**,**b**). The resulting *Gnrh::cre;Dicer*$^{loxP/loxP}$ mice were viable, were born at Mendelian frequencies, and had body weights at adulthood indistinguishable from those of *Dicer*$^{loxP/loxP}$ (wild-type) littermates ($t_{(8)} = 4.35$, $P = 0.390$, $n = 5$ mice). All male and female mutant mice, however, exhibited severe hypogonadism (**Fig. 1b**,**c** and **Supplementary Fig. 2c**,**d**) and sterility ($n = 6$ males; $n = 6$ females) (**Fig. 1d**). Serum levels of the pituitary gonadotropins luteinizing hormone (LH) and follicle-stimulating hormone (FSH)

[1]Inserm, Laboratory of Development and Plasticity of the Neuroendocrine Brain, Jean-Pierre Aubert Research Centre, U1172, Lille, France. [2]University of Lille, FHU 1,000 Days for Health, School of Medicine, Lille, France. [3]Columbia University Medical Center and Berrie Diabetes Center, New York, New York, USA. [4]Department of Cell Biology, Physiology and Immunology, University of Cordoba, Cordoba, Spain. [5]Instituto Maimonides de Investigación Biomédica de Cordoba (IMIBIC/HURS), Cordoba, Spain. [6]CIBER Fisiopatología de la Obesidad y Nutrición, Instituto de Salud Carlos III, Cordoba, Spain. [7]Inserm UMR1141 – PROTECT (Promoting Research Oriented Towards Early CNS Therapies), Paris, France. [8]Present addresses: Endocrinology, Diabetes & Metabolism Service, Centre Hospitalier Universitaire Vaudois, Lausanne, Switzerland, (A.M.) and Centre for Animal Sciences, Central University Punjab, Bathinda, India (J.P.). [9]These authors contributed equally to this work. Correspondence should be addressed to V.P. (vincent.prevot@inserm.fr).

Received 22 February; accepted 1 April; published online 2 May 2016; corrected after print 3 June 2016; doi:10.1038/nn.4298

were markedly reduced in both female and male adults (**Fig. 1e**,**f**). LH levels were readily increased by systemic GnRH injection, demonstrating intact pituitary function in *Gnrh::cre;Dicer*$^{loxP/loxP}$ mice (**Supplementary Fig. 2e**), but were unaffected by the intracerebroventricular infusion of two potent stimulators of the GnRH system that trigger LH release in wild-type males: kisspeptin, which acts through its receptor Gpr54, and NMDA, which bypasses the kisspeptidergic system to stimulate GnRH neurons[10,11] (**Supplementary Fig. 2f**,**g**), suggesting that the hypogonadotropic hypogonadism observed was due primarily to hypothalamic GnRH deficiency. This possibility was further supported by the effective promotion of uterine growth (**Supplementary Fig. 2c**) and ovulation (**Supplementary Fig. 2h**) by treatment with gonadal steroids and pregnant mare gonadotropins, respectively, in *Gnrh::cre;Dicer*$^{loxP/loxP}$ mice, indicating that gonadal function could be fully rescued by hormonal replacement downstream of GnRH neurons. While some female *Gnrh::cre;Dicer*$^{loxP/loxP}$ mice underwent vaginal opening (5 of 7) (**Fig. 1g**), this external sign of sexual maturation occurred significantly later than in *Dicer*$^{loxP/loxP}$ mice (Breslow-Wilcoxon test: $\chi^2_{(2)} = 9.363$, $P = 0.0022$, $n = 5$ and 11 mice per group), and the absence of estrous cyclicity in vaginal smears showed that they never ovulated ($n = 7$ mice) (**Fig. 1h**) despite normal somatic growth (two-way repeated-measures ANOVA, genotype: $F_{(1,8)} = 0.0129$, $P = 0.912$; time: $F_{(11,88)} = 178.9$, $P < 0.0001$; interaction: $F_{(11,88)} = 5.19$, $P < 0.0001$; subject matching: $F_{(8,88)} = 104$, $P = 0.0001$, $n = 5$ mice per group) (**Fig. 1i**). Similarly, male *Gnrh::cre;Dicer*$^{loxP/loxP}$ mice ($n = 5$) did not exhibit balanopreputial separation, which occurred at 34.9 ± 1.8 days of age in *Dicer*$^{loxP/loxP}$ littermates ($n = 11$), or spermatozoa in seminiferous tubules (**Fig. 1c**).

Following these physiological data, neuroanatomical analyses revealed a complete absence of GnRH immunoreactivity in the hypothalamus of adult male and female mutants (**Fig. 2a** and **Supplementary Fig. 3**), reminiscent of Kallmann syndrome in humans[2], in which GnRH neurons originating in the olfactory placode fail to migrate into the brain during development. To determine whether *Dicer* invalidation in mouse GnRH neurons similarly affected their migration, we examined them on embryonic day (E) 14.5, when half the migrating GnRH neurons are still in the nose, and at postnatal day (P) 0, when GnRH neurons have completed their migration into the hypothalamic preoptic region, their principal site of residence, and sent projections to the median eminence where they release their neurohormone into portal capillaries for delivery to the anterior pituitary[12,13]. Unlike what is seen in humans with Kallmann syndrome, GnRH neurons displayed no migratory defects and GnRH immunoreactivity was comparable in *Gnrh::cre;Dicer*$^{loxP/loxP}$ and *Dicer*$^{loxP/loxP}$ littermates at P0 ($t_{(4)} = 0.27$, $P = 0.8$, $n = 3$ mice per group) (**Supplementary Fig. 4**). GnRH deficiency in mutant mice was thus not due to a developmental lack of GnRH neurons, but acquired postnatally.

Hypothalamic GnRH peptide content increases progressively between birth and puberty, quickening markedly during the infantile period (P7–P20)[14,15]. We thus examined hypothalamic GnRH immunoreactivity at different postnatal ages and found that its disappearance in *Gnrh::cre;Dicer*$^{loxP/loxP}$ mice occurred gradually in both sexes, starting during the infantile period (**Fig. 2a** and **Supplementary Fig. 5**) and accelerating during the juvenile period after weaning; i.e., P21 to ~P35 (two-way ANOVA: genotype, $F_{(1,45)} = 84.05$, $P < 0.0001$; time, $F_{(4,45)} = 19.56$, $P < 0.0001$; interaction, $F_{(4,45)} = 6.62$, $P = 0.0003$; Sikad's multiple comparison test, *Dicer*$^{loxP/loxP}$ versus *Gnrh::cre;Dicer*$^{loxP/loxP}$: $t_{(45)} = 0.624$, $P = 0.978$, $n = 3$ per group at P0; $t_{(45)} = 2.12$, $P = 0.184$, $n = 5$ and 7, respectively, at P12; $t_{(45)} = 5.31$, $P < 0.0001$, $n = 6$ and 7 at P21; $t_{(45)} = 7.98$, $P < 0.0001$, $n = 7$ and 9 at P28; and $t_{(45)} = 6.32$, $P < 0.0001$, $n = 4$ per group in adults) (**Fig. 2a** and **Supplementary Fig. 5**). Given the GnRH peptide's extreme stability (for instance, GnRH immunoreactivity persists in axon terminals days after its disappearance from the cell body; see **Supplementary Fig. 5**), we decided to construct a reporter system to more accurately track GnRH-expressing neurons postnatally. The generation of *Gnrh::cre;Dicer*$^{loxP/loxP}$*;tdTomato*$^{loxP/STOP}$ trigenic mice showed that GnRH neurons did not die in the absence of miRNAs but simply lost GnRH immunoreactivity (**Fig. 2b**). In these mice, in which tdTomato, once triggered by *Gnrh* transcriptional activation and thus Cre production during development, is expressed constitutively in GnRH neurons even without continued *Gnrh* promoter activity, the number of tdTomato-expressing GnRH neurons did not significantly decrease. However, around ~70% of them had lost GnRH peptide at P21 when compared to *Gnrh::cre;Dicer*$^{+/+}$*;tdTomato*$^{loxP/STOP}$ littermates. To further pinpoint the stage at which GnRH expression is blocked in *Dicer*-deficient mice, we constructed *Gnrh::Gfp;Gnrh::cre;Dicer*$^{loxP/loxP}$ reporter mice, which express GFP under the control of an ectopic *Gnrh* promoter only when the promoter is currently active, unlike tdTomato in the previous experiment. These mice showed a concomitant loss of GnRH peptide and GFP during postnatal development (**Supplementary Fig. 6**). Because the 3′ UTR, and thus the putative miRNA target sequence, of the *Gfp* transcript is completely distinct from the one encoding *Gnrh*, this indicates that miRNAs probably did not regulate *Gnrh* transcript stability and/or translation directly but rather affected genes necessary for *Gnrh* transcription, such as promoter modulators.

An infantile miRNA switch inverts *Gnrh* promoter modulator expression

To tease apart the mechanism of miRNA action, we next verified the expression profile of the *Gnrh* transcript as well as of *Gnrh* promoter modulators in GnRH neurons isolated by fluorescence-activated cell sorting (FACS) at two stages: P7 and P12. P7 signals the beginning of the infantile period, while at P12 hypothalamic GnRH peptide content undergoes a functionally relevant increase in normal mice[14,15] but begins to decrease in *Dicer*-deficient mice even though most of their GnRH neurons (~80%) still express detectable GFP (**Supplementary Fig. 6**). This increase leads to a phenomenon called 'mini-puberty' in humans, characterized by the first centrally driven, gonad-independent activation of the HPG axis and a significant but transient surge in gonadotropin levels[15,16]. Real-time PCR analyses of FACS-isolated GFP-expressing GnRH neurons from *Gnrh::Gfp;Dicer*$^{loxP/loxP}$ mice (**Fig. 2c** and **Supplementary Fig. 7**), which are wild-type for *Dicer*, revealed a 200% increase in *Gnrh* mRNA between P7 and P12 ($t_{(5)} = -3.20$, $P = 0.024$, $n = 4$ mice per group) (**Fig. 2d**). This was accompanied by an upregulation of mRNA for several promoter activators known to affect GnRH expression[17,18] (**Fig. 2d**) while transcripts of three known GnRH repressors[17,18] remained unchanged (**Fig. 2d**). However, in GnRH neurons lacking *Dicer* (*t*-test, $t_{(5)} = 3.58$, $P = 0.0159$; $n = 4$ mice per group) (**Fig. 2e**) isolated from *Gnrh::Gfp;Gnrh::cre;Dicer*$^{loxP/loxP}$ trigenic mice at P12, when *Gnrh* mRNA should normally begin increasing, *Gnrh* mRNA expression was significantly lower than in neurons from *Dicer* wild-type *Gnrh::Gfp;Dicer*$^{loxP/loxP}$ mice ($t_{(3,12)} = 5.88$, $P = 0.0098$, $n = 4$ per group) (**Fig. 2e**). These altered expression levels were functionally relevant, corresponding to impaired FSH release during the infantile period (females: $t_{(19)} = 5.578$, $P < 0.0001$, $n = 10$ and 11 per group; males: $t_{(20)} = 1.612$, $P = 0.1226$, $n = 12$ and 10 per group) (**Fig. 2f**). In addition to reduced *Gnrh* transcript expression (**Fig. 2e**), there was a marked decrease in the expression of most *Gnrh* promoter activators (**Fig. 3a**) and a 15-fold increase in the *Cebpb* transcript, encoding

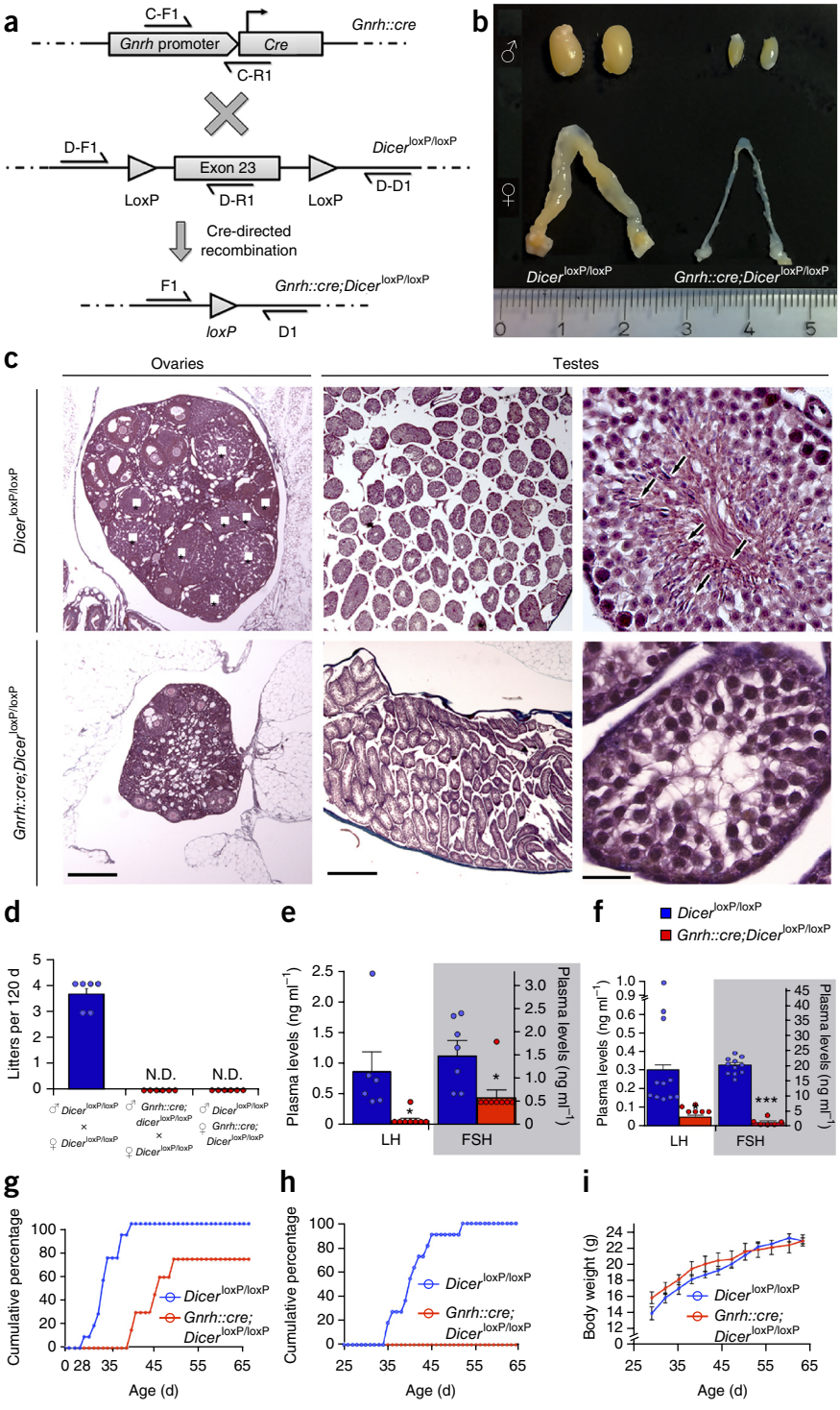

Figure 1 Lack of miRNA biogenesis in GnRH neurons leads to hypogonadotropic hypogonadism and infertility. (**a**) Genetic strategy to invalidate *Dicer* expression specifically in GnRH-expressing cells in mice. D-F1, D-R1, D-D1, C-F1 and C-R1 are primers used for genotyping (see **Supplementary Table 3**). (**b**) Smaller testes and ovaries and thread-like uteri in mutant mice. (**c**) Hematoxylin-eosin-stained ovarian and testicular sections of mutant *Gnrh::cre;Dicer*$^{loxP/loxP}$ mice and their wild-type *Dicer*$^{loxP/loxP}$ littermates. Asterisks show corpora lutea; arrows, spermatozoa. Scale bars: 500 µm (left and middle panels) and 30 µm (right panels). Pictures shown in **b** and **c** are representative of observations in more than 10 animals per sex and per genotype. (**d**) Both male and female *Gnrh::cre;Dicer*$^{loxP/loxP}$ mice are infertile. N.D., not detected. (**e**,**f**) Circulating levels of LH (left panels) and FSH (right panels) in control (blue) and *Dicer* mutants (red): diestrous females (**e**; LH, *t*-test, $t_{(12)} = 2.82$, $P = 0.0155$, $n = 6$ and 8 mice per group; FSH, *t*-test, $t_{(13)} = 2.46$, $P = 0.0287$, $n = 7$ and 8 mice per group) and males (**f**; LH, *t*-test, $t_{(15)} = 2.16$, $P = 0.047$, $n = 6$ and 11 mice per group; FSH, *t*-test, $t_{(15)} = 16.2$, $P < 0.0001$, $n = 6$ and 11 mice per group). (**g**–**i**) While some *Gnrh::cre;Dicer*$^{loxP/loxP}$ female mice undergo vaginal opening during postnatal development (**g**), they never reach puberty (**h**) despite normal somatic growth (**i**). Values shown are means ± s.e.m.

a *Gnrh* promoter repressor (**Fig. 3b**) in *Dicer*-deficient GnRH neurons (**Fig. 3a**,**b**), supporting the hypothesis that miRNAs control *Gnrh* transcript levels indirectly by altering levels of *Gnrh* promoter modulators.

miR-200 and *Zeb1* directly and indirectly control GnRH expression

The altered expression of *Gnrh* promoter activators and repressors suggests that, in the absence of miRNAs, repressors of these activators, in addition to repressors of GnRH itself, might be reciprocally increased. *In silico* analysis of the 3′ UTRs of transcripts encoding these promoter modulators (Aes, Dlx1, Dlx5, Meis1, Otx2, Pbx1, Pknox1, Pouf2f1, Cebpb, Msx1 and Tle4) revealed the presence of putative binding sites for several miRNAs ($P < 0.01$; **Supplementary Table 1**), confirming that miRNAs could regulate their expression. Concordantly, we uncovered an inversion of the expression profile of these and other putative regulatory miRNAs in FACS-sorted wild-type GnRH neurons between P7 and P12 (**Fig. 3c**), which strongly suggests that *Gnrh* promoter activity during the infantile period answers to a miRNA-operated switch. To identify the molecular effectors and targets involved, we looked for miRNAs that were not only differentially expressed between P7 and P12 (**Fig. 3c**) but specifically enriched in GnRH neurons compared to non-GnRH cells at P12 (**Fig. 3d**). Members of the miRNA-200 family, including miR-141 and miR-429 (**Supplementary Fig. 8a**), were among the most highly enriched miRNAs in infantile GnRH neurons when compared to non-GnRH-expressing cells (**Fig. 3d**,**e**). Within this family the expression of miR-200a and miR-429 increased significantly between P7 and P12 (miR-200a, $t_{(4)} = 9.178$, $P = 0.0008$; miR-429, $t_{(5)} = 3.931$, $P = 0.0111$, $n = 3$ and 4 mice per group) (**Fig. 3f**); these miRNAs are known to silence the transcriptional repressor Zeb1 in pituitary gonadotropes, where it regulates LH expression[6]. To verify whether the miR-200–*Zeb1* network[19] (**Supplementary Fig. 8a**) also controlled hypothalamic GnRH expression during postnatal development we analyzed *Zeb1* expression in mice with or

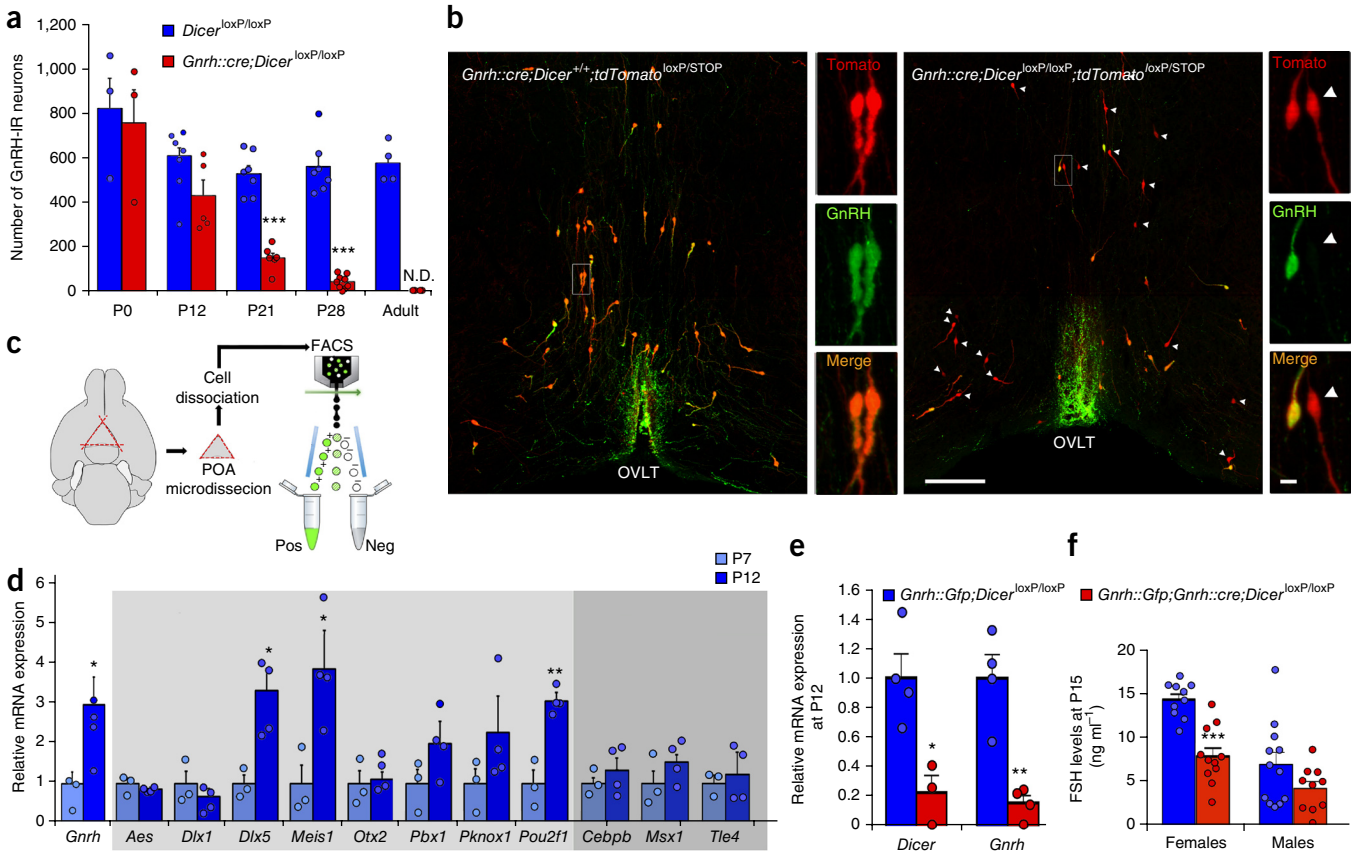

Figure 2 A switch in the control of GnRH gene expression is operated by miRNAs during postnatal developmental. (**a**) Gradual disappearance of GnRH-immunoreactive (GnRH-IR) neurons in *Gnrh::cre;Dicer*$^{loxP/loxP}$ mice (red) during postnatal development. Blue, *Dicer* wild-type. N.D., not detected; ***$P < 0.001$. (**b**) Neuronal lineage tracing shows normal distribution of GnRH neurons in P21 juvenile mice with GnRH deficiency (*Gnrh::cre;Dicer*$^{loxP/loxP}$*;tdTomato*$^{loxP/STOP}$), when compared to control littermates (*Gnrh::cre;Dicer*$^{+/+}$*;tdTomato*$^{loxP/STOP}$). Arrowheads show GnRH-immunonegative, tdTomato-positive neurons. OVLT, organum vasculosum of the lamina terminalis. Scale bars, 200 µm; 10 µm (inset). These images are representative of observations in 3 animals per genotype. (**c**) GnRH-GFP neuron isolation by FACS from the preoptic region of *Gnrh::Gfp* mice. (**d**,**e**) Real-time PCR analysis of expression levels of *Gnrh* mRNA (**d**,**e**), *Dicer* (**e**), and *Gnrh* promoter activators (*t*-test, P7 versus P12, *Aes*, $t_{(5)} = 1.08$, $P = 0.329$; *Dlx1*, $t_{(5)} = 1.22$, $P = 0.277$; *Dlx5*, $t_{(5)} = -3.62$, $P = 0.015$; *Meis1*, $t_{(5)} = -3.17$, $P = 0.024$; *Otx2*, $t_{(5)} = 0.725$, $P = 0.500$; *Pbx1*, $t_{(5)} = 1.83$, $P = 0.126$; *Pknox1*, $t_{(5)} = 1.42$, $P = 0.216$; *Pou2f1*, $t_{(5)} = -6.14$, $P = 0.0017$; *Cebpb*, $t_{(5)} = 0.83$, $P = 0.444$; *Msx1*, $t_{(5)} = 0.702$, $P = 0.514$; *Tle4*, $t_{(5)} = 0.61$, $P = 0.566$; $n = 3$ and 4 mice per group) (light gray shaded area in **d**) and repressors (dark gray shaded area in **d**) in FACS-sorted GnRH-GFP neurons. *$P < 0.05$; **$P < 0.01$. Values are expressed relative to P7 or wild-type values, as appropriate, set at 1. (**f**) FSH levels in females (*t*-test, $t_{(19)} = 5.58$, $P < 0.0001$, $n = 10$ and 11 animal per group) and males (*t*-test, $t_{(20)} = 1.61$, $P = 0.123$, $n = 10$ and 12 mice per group) at P15. Values shown are means ± s.e.m.

without miRNA production in GnRH neurons. Not only was *Zeb1* mRNA expressed in infantile GnRH neurons, its expression also decreased significantly between P7 and P12 in *Gnrh::Gfp;Dicer*$^{+/+}$ mice ($t_{(6)} = 4.86$, $P = 0.0028$, $n = 4$ per group) (**Fig. 4a**). Real-time PCR in GnRH neurons isolated from *Gnrh::Gfp;Gnrh::cre;Dicer*$^{loxP/loxP}$ and *Gnrh::Gfp;Dicer*$^{loxP/loxP}$ littermates at P12 further showed that *Zeb1* mRNA was significantly upregulated in mice with *Dicer*-deficient GnRH neurons ($t_{(5)} = -3.38$, $P = 0.0195$, $n = 3$ and 4 mice per group) (**Fig. 4b**). *In silico* sequence analysis revealed varying numbers of putative Zeb1-binding sites in the genes of all *Gnrh* transcriptional activators examined (**Supplementary Fig. 8b**), including *Pou2f1*, which, in addition to activating the *Gnrh* gene directly, could increase miR-200 levels[20] and thereby indirectly influence *Gnrh* activation by repressing Zeb1. Concordantly, we found that both human (**Supplementary Fig. 8c**) and mouse *Gnrh* promoters (**Fig. 4c**) contained putative Zeb1-binding sites. Chromatin immunoprecipitation assays in an immortalized mouse GnRH neuronal cell line expressing both promoters (**Fig. 4c** and **Supplementary Fig. 8c**) revealed that several predicted as well as previously unknown sites were functionally active.

Taken together, these data support the idea that increased Zeb1 expression in the absence of miRNA biogenesis could mediate the downregulation of these activators and of GnRH in these neurons (**Fig. 3a**). To test this hypothesis, we infused a target-site blocker, TSB-200, into the brains of *Gnrh::Gfp;Dicer*$^{+/+}$ mice to selectively hamper miR-200b, miR-200c and miR-429 (miR-200b/200c/429) binding to *Zeb1* mRNA (**Supplementary Fig. 8d**). TSBs are small, freely diffusible locked-nucleic-acid oligonucleotides with two notable characteristics: (i) they are highly stable (with a reported half-life *in vivo* on the order of weeks) and resistant to nuclease-mediated degradation *in vitro* and *in vivo*, thanks to their modified phosphorothioate backbone[21], and (ii) they are complementary to both the miRNA and the binding site being targeted, making them extremely specific (see, for example, **Supplementary Fig. 9b–e**). As shown by fluorescence-tagged sequences (**Supplementary Fig. 9a**), TSBs readily targeted the preoptic region and GnRH neurons 72 h after infusion into the lateral ventricle of *Gnrh::Gfp;Dicer*$^{+/+}$ pups. TSB-200 significantly increased *Zeb1* mRNA levels in FACS-sorted GFP-positive GnRH neurons at P12 as compared to a scrambled sequence (*t*-test,

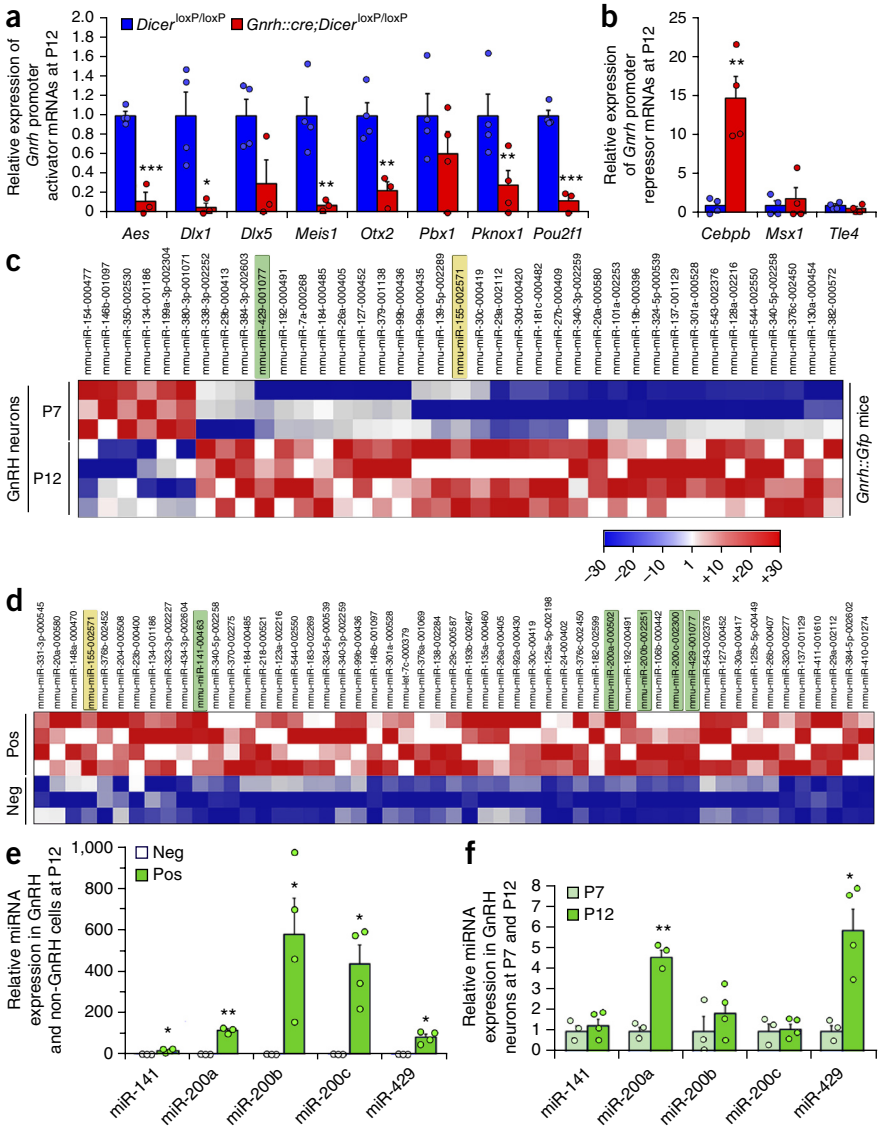

Figure 3 miRNAs regulate the expression of *Gnrh* promoter modulators in infantile GnRH neurons. (**a**,**b**) RT-PCR analysis of the expression of *Gnrh* promoter activators (**a**) and repressors (**b**) in FACS-sorted GnRH-GFP neurons from mice selectively lacking *Dicer* in GnRH neurons (red bars) or wild-type for *Dicer* (blue bars) All values are expressed relative to wild-type values, set at 1 (*t*-test, $Dicer^{loxP/loxP}$ versus $Gnrh::cre;Dicer^{loxP/loxP}$; **a**: *Aes*, $t_{(5)} = 9.58$, $P = 0.0002$; *Dlx1*, $t_{(5)} = 3.78$, $P = 0.032$; *Dlx5*, $t_{(5)} = 2.41$, $P = 0.061$; *Meis1*, $t_{(5)} = 4.00$, $P = 0.018$; *Otx2*, $t_{(5)} = 4.34$, $P = 0.0074$; *Pbx1*, $t_{(6)} = 1.21$, $P = 0.271$; *Pknox1*, $t_{(6)} = 2.63$, $P = 0.039$; *Pou2f1*, $t_{(5)} = 10.00$, $P = 0.0002$; $n = 3$ and 4 mice per group; **b**: *Cebpb*, $t_{(6)} = 4.79$, $P = 0.003$; *Msx1*, $t_{(6)} = 0.537$, $P = 0.61$; *Tle4*, $t_{(6)} = 1.22$, $P = 0.27$, $n = 4$ animal per group) ($^*P < 0.05$; $^{**}P < 0.01$; $^{***}P < 0.001$). (**c**,**d**) All miRNAs whose expression levels in GnRH neurons change between P7 and P12, organized according to the direction of the change (**c**), and miRNAs (including family members of those identified in **c**) that are specifically enriched in GnRH neurons as compared to surrounding non-GnRH cells at P12 (**d**). See also **Supplementary Table 5**. Pos, GFP-expressing neurons; Neg, GFP-negative cells. ΔΔCT (threshold cycle) analyses were performed using GnRH neurons (Pos) at P7 as the control group in **c** and using non-GnRH cells (Neg) at P12 as the control group in **d**. Shades of blue indicate a decrease in expression compared to control; shades of red, an increase. (**e**,**f**) RT-PCR analysis of the expression of miR-200 family members in FACS-sorted cells from the preoptic region microdissected from *Gnrh::Gfp* mice wild-type for *Dicer* either at P12 (**e**; *t*-test, Pos versus Neg: miR-141, $t_{(5)} = 3.37$, $P = 0.0199$; miR-200a, $t_{(4)} = 13.57$, $P = 0.0002$; miR-200b, $t_{(5)} = 2.775$, $P = 0.0391$; miR-200c, $t_{(5)} = 4.016$, $P = 0.0102$; miR-429, $t_{(5)} = 4.778$, $P = 0.005$; $n = 3$ and 4 mice per group) or at P7 and P12 (**f**; *t*-test, P7 versus P12: miR-141, $t_{(5)} = 0.6652$, $P = 0.5354$; miR-200a, $t_{(4)} = 9.178$, $P = 0.0008$; miR-200b, $t_{(5)} = 0.9572$, $P = 0.3824$; miR-200c, $t_{(5)} = 0.2604$, $P = 0.805$; miR-429, $t_{(5)} = 3.931$, $P = 0.011$; $n = 3$ and 4 animal per group). Values shown are means ± s.e.m.

$t_{(9)} = -3.33$, $P = 0.0087$, $n = 5$ and 6 mice per group) (**Fig. 4d**) but did not affect the transcripts for two other miR-200b/200c/429 target genes, *Lpin1* (*t*-test, $t_{(10)} = 0.663$, $P = 0.52$, $n = 6$ per group)[22] and *Maf* (*t*-test, $t_{(10)} = -0.192$, $P = 0.85$, $n = 6$ per group)[23] (**Fig. 4d**). This increased *Zeb1* expression was specific to GnRH neurons (**Supplementary Fig. 10c**), in keeping with the enrichment of miR-200b/200c/429 in these cells (**Fig. 3d**,**e**), and was accompanied by a significant decrease in transcripts of two *Gnrh* promoter activators that were also upregulated in GnRH neurons at P12 compared to P7 (**Fig. 2d**), *Meis1* (*t*-test, $t_{(8)} = 2.53$, $P = 0.035$, $n = 4$ and 6 mice per group) and *Pou2f1* (*t*-test, $t_{(10)} = 4.15$, $P = 0.002$, $n = 6$) (**Fig. 4e**); promoter activator transcripts *Aes*, *Otx2*, *Pbx1* and *Pknox1*, which did not significantly change between P7 and P12, were also unchanged by TSB-200 infusion. These genes also had fewer putative Zeb1-binding sites than those whose expression was strongly modified by altered *Zeb1* expression (**Supplementary Fig. 8b**). As expected, *Gnrh* transcription was also downregulated by the blockade of miR-200–*Zeb1* binding at P12 (*t*-test, $t_{(9)} = 5.37$, $P = 0.0004$, $n = 4$ and 7 mice per group) (**Fig. 4f**). This repression of *Gnrh* was apparently mediated by the inhibition of *Gnrh* promoter activity, as shown by the strong decrease in *Gfp* reporter mRNA expression (*t*-test, $t_{(10)} = 14.1$, $P < 0.0001$, $n = 6$ mice per group) (**Fig. 4f**), suggesting that the miR-200–*Zeb1* network is actively involved in the switch in *Gnrh* transcriptional control in the infantile mouse hypothalamus (**Supplementary Fig. 8e**).

Hampering miR-155 and *Cebpb* binding lowers *Gnrh* mRNA

Contrary to the downregulation of *Gnrh* promoter activators in mice with *Dicer*-deficient GnRH neurons, the mRNA for a GnRH repressor, *Cebpb*, which encodes CAAT/enhancer binding protein β (C/EBPβ), was highly upregulated (**Fig. 3b**). We thus reasoned that C/EBPβ repression by miRNAs would be greater in infantile wild-type mice. The miRWalk database, which provides validated information on miRNA–target interactions[24], showed that among miRNAs upregulated in GnRH neurons at P12 (**Fig. 3c**,**d**) was miR-155, whose seed target region is present in the *Cebpb* transcript 3′ UTR ($P = 0.0077$, **Supplementary Table 2** and **Supplementary Fig. 9b**,**c**)[25]. To determine whether the tenfold increase in miR-155 expression between P7 and P12 ($t_{(4)} = -4.85$, $P = 0.0083$, $n = 3$ mice per group) (**Fig. 5a**) actually

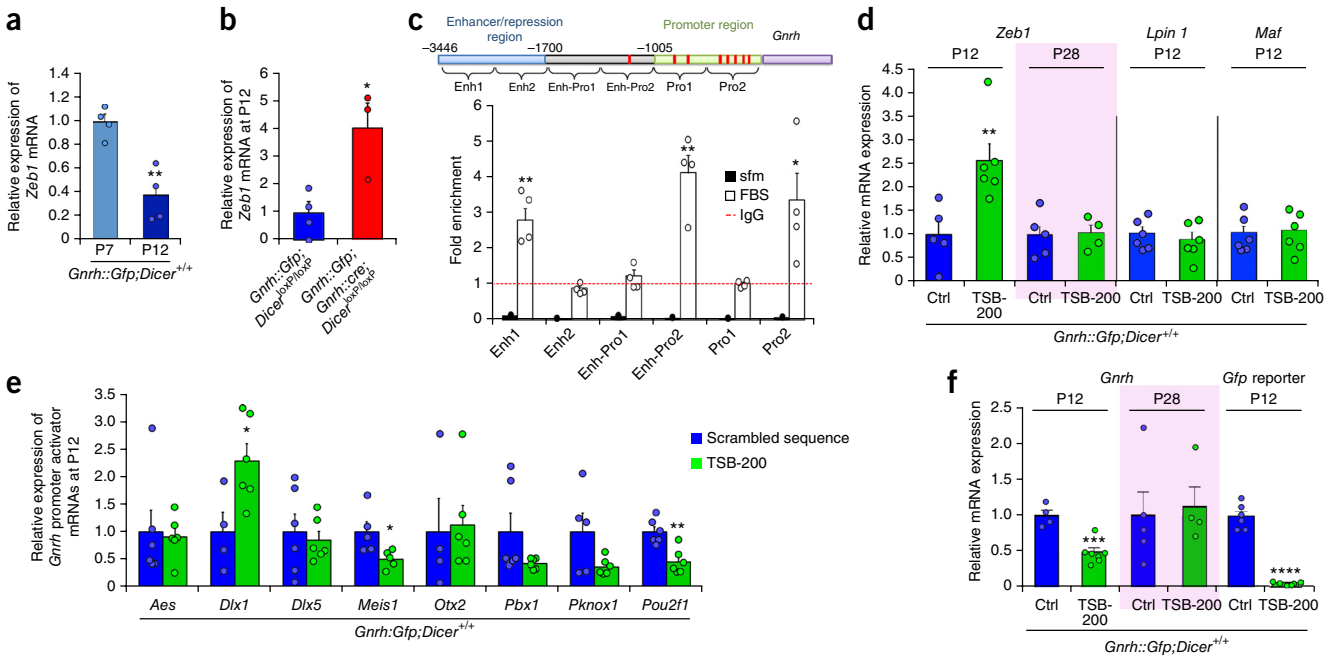

Figure 4 Knocking down the ability of miR-200 to repress *Zeb1* expression in the brain alters infantile *Gnrh* promoter activity and *Gnrh* mRNA expression. (**a**,**b**) RT-PCR analysis of the expression of *Zeb1* in GnRH-GFP neurons isolated from *Gnrh::Gfp;Dicer*$^{+/+}$ mice at P7 and P12 (**a**) or from mice in which *Dicer* expression is invalidated or not in GnRH neurons (**b**). (**c**) Diagram showing the distribution of putative *Zeb1* binding sites on the mouse *Gnrh* gene (upper panel) and their validation using a Zeb1 chromatin immunoprecipitation assay in an immortalized mouse cell line secreting GnRH and cultured in the presence or absence of fetal bovine serum (FBS). Values are expressed relative to the immunoprecipitation of chromatin containing the *Gnrh* promoter region with irrelevant IgG species, arbitrarily set at 1 (dotted red line). Enh, enhancer; Pro, promoter. *t*-test, serum-free medium (sfm) versus FBS: *Enh1*, $t_{(6)} = 4.756$, $P = 0.0031$; *Enh2*, $t_{(6)} = 2.320$, $P = 0.0595$; *Enh-Pro1*, $t_{(6)} = 0.9063$, $P = 0.3997$; *Enh-Pro2*, $t_{(6)} = 5.462$, $P = 0.0016$; *Pro1*, $t_{(6)} = 0.2104$, $P = 0.8403$; *Pro2*, $t_{(6)} = 2.467$, $P = 0.0486$, $n = 4$ mice per group. (**d**–**f**) Effect of the intracerebroventricular (i.c.v.) injection of TSB-200 (green bars) or a scrambled sequence (Ctrl, blue bars) on the expression of *Zeb1*, *Lpin1* and *Maf* (**d**), mRNA for *Gnrh* promoter activators (*t*-test, control versus TSB-200: *Aes*, $t_{(10)} = 0.22$, $P = 0.823$; *Dlx1*, $t_{(8)} = 2.63$, $P = 0.03$; *Dlx5*, $t_{(10)} = 0.43$, $P = 0.67$; *Otx2*, $t_{(8)} = 0.183$, $P = 0.0859$; *Pbx1*, $t_{(10)} = 1.69$, $P = 0.12$; *Pknox1*, $t_{(9)} = -2.024$, $P = 0.074$, $n = 4$ and 6 animals per group) (**e**), and *Gnrh* transcript and *Gnrh* promoter activity (**f**) in GnRH-GFP neurons. White zones show data from mice at P12. Pink zones show data from P28 mice. Values are expressed relative to P7, wild-type or control values, as appropriate, set at 1. (*$P < 0.05$; **$P < 0.01$; ***$P < 0.001$; ****$P < 0.0001$). Values shown are means ± s.e.m.

regulates C/EBPβ expression in GnRH neurons, we used TSB-155 to selectively hamper miR-155–*Cebpb* binding in the hypothalamus of infantile mice (**Supplementary Fig. 9d**,**e**). TSB-155 infusion into *Gnrh::Gfp;Dicer*$^{+/+}$ mice markedly increased *Cebpb* mRNA levels in GnRH neurons when compared to a scrambled sequence ($t_{(9)} = -3.41$, $P = 0.0038$, $n = 5$ and 6 mice per group) (**Fig. 5b**), but did not change mRNA levels of *Lpin1* ($t_{(10)} = 0.601$, $P = 0.56$, $n = 6$) or *Maf* ($t_{(10)} = 0.406$, $P = 0.69$, $n = 6$) (**Fig. 5b**), which are also validated miR-155 targets[26,27]. This TSB-155–mediated upregulation of the *Cebpb* transcript was associated with a strong inhibition of both *Gnrh* promoter activity, as indicated by *Gfp* mRNA levels ($t_{(10)} = 14.0$, $P < 0.0001$, $n = 6$ mice per group) (**Fig. 5c**), and *Gnrh* mRNA levels ($t_{(8)} = 3.57$, $P = 0.0073$, $n = 4$ and 6 mice per group) (**Fig. 5c**). However, using ChIPBase (an integrated resource and platform for decoding transcription factor binding maps on the basis of chromatin immunoprecipitation and sequencing (ChIP-seq) data[28]), we found that the *Zeb1* gene contained binding sites for C/EBPβ in six different regulatory regions[29,30] (**Supplementary Fig. 11a**), but no binding site for miR-155, suggesting that C/EBPβ could regulate *Gnrh* mRNA levels indirectly, as well as directly, by influencing *Zeb1* expression. In agreement with this hypothesis, TSB-155, which selectively upregulates *Cebpb* expression, also increased the *Zeb1* transcript in *Dicer*$^{+/+}$ GnRH neurons ($t_{(9)} = -2.89$, $P = 0.0177$, $n = 5$ and 6 per group) (**Fig. 5c**). Furthermore, *in silico* and ChIP-seq analyses revealed several binding sites for both C/EBPβ and Zeb1 on the *Gpr54* gene (**Supplementary Figs. 8b** and **11b**), suggesting that in addition to their direct and promoter-activator–mediated effects, C/EBPβ and Zeb1 could repress *Gnrh* gene transcription indirectly by blocking kisspeptidergic signaling through Gpr54, which is known to increase *Gnrh* transcription by promoting the nuclear translocation of the *Gnrh* promoter activator Otx2 (ref. 31 and **Supplementary Fig. 11c**). Supporting this hypothesis, real-time PCR analysis revealed that in animals with Dicer-deficient GnRH neurons, *Gpr54* mRNA levels were also strongly reduced ($t_{(6)} = 4.22$, $P = 0.0056$, $n = 4$ mice per group) (**Fig. 5d**), to a similar extent as that of other GnRH activators (**Fig. 3a**).

Blocking infantile nitric oxide release partially rescues GnRH expression

C/EBPβ is also known to mediate the nitric oxide (NO)-induced repression of *Gnrh* expression[17]. However, we have recently shown that activation of neuronal NO synthase (nNOS) in preoptic neurons, itself regulated by Kisspeptin-Gpr54 binding[32], is required for sexual maturation[33]. In wild-type mice in the present study, nNOS activation by its phosphorylation at Ser1412 (p-nNOS) (ref. 34) increased significantly in the preoptic region between P7 and P12, when GnRH neuronal network synaptic connectivity is being established[35,36] (p-nNOS/nNOS ratio, Mann-Whitney test: $U = 0$, $P = 0.0286$, $n = 4$ animals per group) (**Fig. 5e**). To determine whether the marked decrease in GnRH expression in *Dicer*-deficient mice could be related to this infantile increase in NO-C/EBPβ signaling, we next treated P12 *Gnrh::Gfp;Gnrh::cre;Dicer*$^{loxP/loxP}$ mice with the NOS inhibitor *N*-G-nitro-L-arginine methyl ester (L-NAME; 50 mg/kg, given

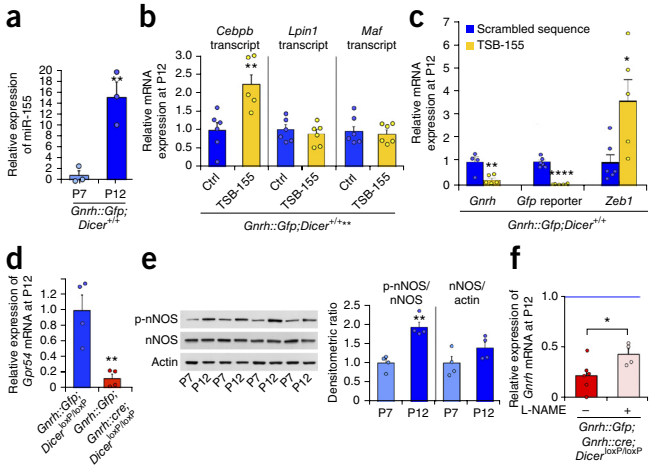

Figure 5 miR-155 modulates *Cebpb*, *Gnrh* and *Zeb1* mRNA expression in infantile GnRH neurons. (**a**) RT-PCR analysis of the expression of miR-155 in FACS-isolated GnRH-GFP neurons between P7 and P12 (**$P < 0.01$). (**b**,**c**) Effect of the i.c.v. injection of TSB-155 (yellow bar) or a scrambled sequence (Ctrl, blue bar) on the expression of *Cebpb*, *Lpin1* and *Maf* (**b**), and on *Gnrh* promoter activity, and GnRH and *Zeb1* (**c**) transcripts in GnRH-GFP neurons of infantile mice. (**d**) RT-PCR analysis of expression levels of *Gpr54* mRNA in FACS-sorted GnRH-GFP neurons (**$P < 0.01$). (**e**) Western blot and quantitative comparison of phosphorylated and total nNOS protein expression in the preoptic region of wild-type mice between P7 and P12 ($n = 3$ per age). Actin was used as a loading control to ensure that equal amounts of proteins were loaded for P7 and P12. Values are expressed relative to P7, set at 1. Full-length blots are presented in **Supplementary Figure 15**. (**f**) L-NAME treatment partially rescues *Gnrh* mRNA expression in P12 mice harboring a *Dicer* deficiency in GnRH neurons. *Gnrh* mRNA levels were arbitrarily set at 1 in control P12 $Dicer^{loxP/loxP}$ mice (blue line). (*$P < 0.05$; ****$P < 0.0001$). Values are expressed relative to untreated wild-type values, set at 1. Values shown are means ± s.e.m.

intraperitoneally) and assessed *Gnrh* mRNA expression in FACS-isolated neurons 12 h later. Reduced NO production following L-NAME treatment partially but significantly rescued *Gnrh* transcript levels ($t_{(8)} = -2.40$, $P = 0.043$, $n = 6$ and 7 mice per group) (**Fig. 5f**). In addition to the alleviation of the previously demonstrated repressive effect of C/EBPβ on the *Gnrh* promoter[17], the increased GnRH expression could have resulted from the inhibition of the transcriptional activation of Zeb1 by C/EBPβ (**Supplementary Fig. 11a**), as indicated by the 2.4-fold increase in transcripts for Pou2f1 (in L-NAME-injected versus saline-injected mice; *t*-test: $t_{(9)} = 2.92$, $P = 0.017$, $n = 5$ and 6 per group; **Supplementary Fig. 9f**). Increased NO levels during this period crucial for subsequent GnRH neuronal function might therefore actually participate in the multilayered transcriptional repression of the *Gnrh* gene in the absence of post-transcriptional silencing of C/EBPβ by miRNAs (**Supplementary Fig. 9g**). In other words, not only do miRNAs control reproductive capacity by controlling the switch in *Gnrh* promoter activity in infantile GnRH neurons, they do so through an intricate mechanism involving crosstalk between inductive and repressive pathways.

miR-200 family and *Zeb-1* binding controls GnRH function

To assess the functional involvement of miR-200 family members and miR-155 in GnRH neurons in puberty onset, we performed a single-bolus injection of the same TSB-200 and/or TSB-155 into the brains of female wild-type mice at P9 and monitored sexual maturation after weaning. Fluorescently labeled TSBs were detectable in the brain up to 2 weeks after injection (**Supplementary Fig. 9a**), in keeping with previous reports showing that they remained active for at least a week *in vivo*[37]. While growth (**Supplementary Fig. 12a**) was similar in TSB- and scrambled-sequence-injected mice, TSB-injected mice exhibited a precocious onset of puberty when compared to control mice (**Fig. 6a**). This effect was most pronounced in TSB-200–infused mice, with 50% of animals displaying their first estrus by P32; i.e., more than 10 d before control mice. In line with these results, TSB-200–infused mice showed significantly elevated peripubertal afternoon surges of plasma LH at P38, while changes in LH levels induced by TSB-155 treatment did not reach statistical significance when compared to control mice, in which plasma LH levels were at the limit of detection (**Fig. 6b**). The combination of TSB-200 and TSB-155, however, only minimally increased LH levels (**Fig. 6b**; one-way ANOVA: $F_{(3,32)} = 3.475$, $P = 0.0272$, $n = 8$, 9, 9 and 10 mice per group; Tukey's multiple comparisons test: control versus treated groups: TSB-200, $q_{(32)} = 4.03$, $P = 0.0361$; TSB-155, $q_{(32)} = 1.4$, $P = 0.754$; TSB-200+TSB-155, $q_{(32)} = 0.151$, $P = 0.9996$), and induced earlier puberty onset by about 5 d when compared to control mice, similarly to TSB-155 treatment alone (**Fig. 6a**; Breslow-Wilcoxon test: TSB vs. control treatment: TSB-200, $\chi^2_{(1)} = 10.86$, $P = 0.01$; TSB-155, $\chi^2_{(1)} = 5.181$, $P = 0.0228$; TSB-200+155, $\chi^2_{(1)} = 5.797$, $P = 0.0161$, $n = 8$, 9, 9 and10 mice per group). To verify whether this discrepancy in the impact of blocking miR-200 and miR-429 (miR-200/429) binding to *Zeb1* mRNA versus miR-155–*Cebpb* binding on *Gnrh* promoter activity at P12 (**Figs. 4f** and **5c**, respectively) and on subsequent sexual maturation (**Fig. 6a**) was linked to differences in the specific cell types targeted by TSB-155 and TSB-200 in the hypothalamus, we analyzed the effects of TSB injection on *Cebpb* and *Zeb1* expression in non-GnRH cells at P12. In agreement with the enrichment of miRNA expression in GnRH neurons compared to non-GnRH hypothalamic cells, which is about 50-fold higher for miR-200/429 (**Fig. 3e**) than for miR-155 (**Supplementary Fig. 10a**), *Cebpb* mRNA levels were significantly increased in non-GnRH cells of the preoptic region after TSB-155 infusion (**Supplementary Fig. 10b**), while TSB-200 treatment altered neither *Cebpb* nor *Zeb1* transcripts in these cells (**Supplementary Fig. 10b**,**c**). In contrast to TSB-155, therefore, TSB-200 selectively targets GnRH neurons. Altogether, these data suggest that, in keeping with the complex feedback mechanisms at work (**Supplementary Fig. 13**), selectively blocking GnRH production in an excessive manner (**Fig. 4f**) and then releasing the block prematurely can trigger precocious puberty, possibly because of a rebound effect (**Supplementary Fig. 12b**). In line with this hypothesis, in females treated with TSB-200 at P9, there was a normalization of the levels of *Zeb1* mRNA ($t_{(7)} = 0.0797$, $P = 0.939$, $n = 4$ and 5 mice per group) (**Fig. 4d**) and *Gnrh* mRNA levels ($t_{(7)} = 0.3079$, $P = 0.767$, $n = 4$ and 5 per group) (**Fig. 4f**) in FACS-sorted GnRH neurons at P28 (i.e., shortly before the observed date of puberty onset), accompanied by a significant elevation in afternoon circulating levels of LH, when compared with control female mice ($t_{(8)} = 2.344$, $P = 0.0471$, $n = 4$ and 6 per group) (**Fig. 6c**).

To determine whether the miR-200–*Zeb1* network could also control GnRH function outside of this critical infantile time-window leading up to puberty, we next infused TSB-200 into the hypothalamic preoptic region of cycling adult female mice and followed their estrous cycles (**Fig. 6d**). While scrambled-sequence–infused control mice did not exhibit any marked alteration of their estrous cycles, most mice treated with TSB-200 (5 out of 6) showed a slight prolongation in the number of days spent in diestrus (a basal stage when LH is released at nadir levels) and eventually reached proestrus (when the preovulatory surge of LH occurs) but displayed an incomplete cycle at least once during the first 2 weeks after injection (**Fig. 6d**). In line with this observation,

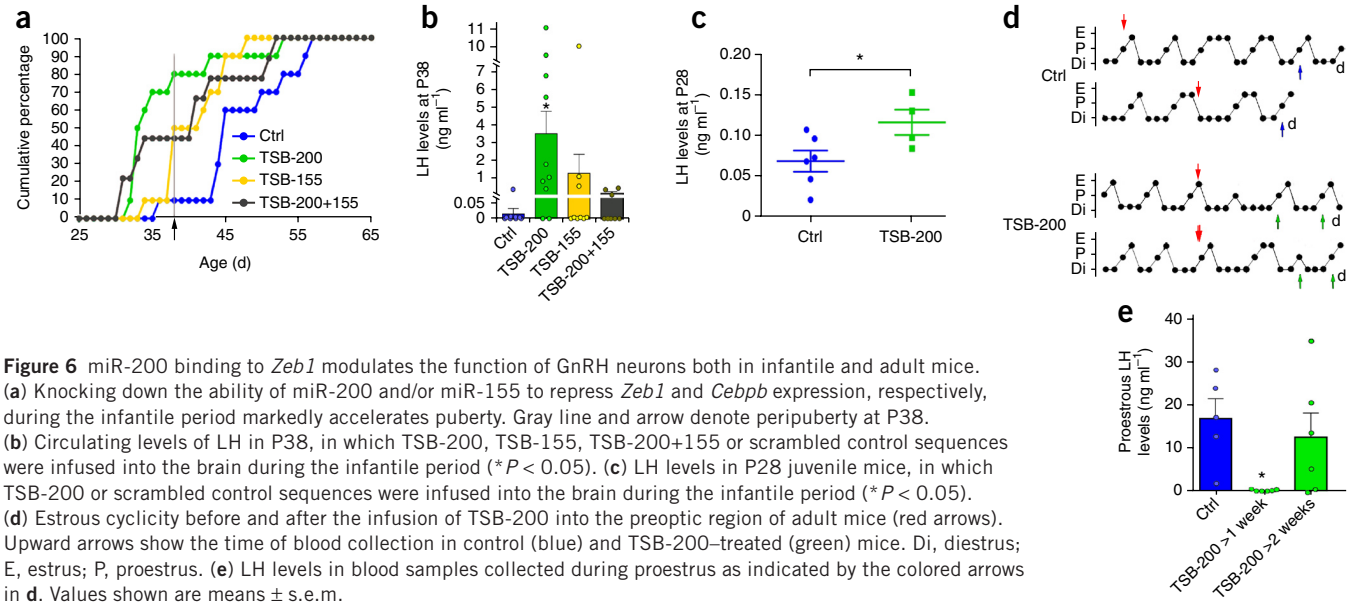

Figure 6 miR-200 binding to *Zeb1* modulates the function of GnRH neurons both in infantile and adult mice. (**a**) Knocking down the ability of miR-200 and/or miR-155 to repress *Zeb1* and *Cebpb* expression, respectively, during the infantile period markedly accelerates puberty. Gray line and arrow denote peripuberty at P38. (**b**) Circulating levels of LH in P38, in which TSB-200, TSB-155, TSB-200+155 or scrambled control sequences were infused into the brain during the infantile period (*$P < 0.05$). (**c**) LH levels in P28 juvenile mice, in which TSB-200 or scrambled control sequences were infused into the brain during the infantile period (*$P < 0.05$). (**d**) Estrous cyclicity before and after the infusion of TSB-200 into the preoptic region of adult mice (red arrows). Upward arrows show the time of blood collection in control (blue) and TSB-200–treated (green) mice. Di, diestrus; E, estrus; P, proestrus. (**e**) LH levels in blood samples collected during proestrus as indicated by the colored arrows in **d**. Values shown are means ± s.e.m.

proestrous LH levels 1 week after injection showed a characteristic surge in controls but not in TSB-200-treated mice (**Fig. 6e**; one-way ANOVA: $F_{(2,14)} = 4.371$, $P = 0.0335$, $n = 5$ and 6 mice per group; control versus TSB-200 >1 week, $q_{(14)} = 3.956$, $P = 0.0357$; control versus TSB-200 >2 weeks, $q_{(14)} = 1.02$, $P = 0.754$). In 4 of the 6 animals treated with TSB-200, LH levels recovered and displayed normal preovulatory surges by the third week after TSB infusion (**Fig. 6e**).

DISCUSSION

The balance between inductive and repressive signals is a process essential for successful reproduction in mammals[38,39]. Our data provide the first physiological and neuroanatomical evidence that miRNAs, by modulating this balance in the GnRH gene network during the infantile period, are essential to the postnatal development of the hypothalamic neuroendocrine neurons controlling the onset of puberty and fertility in mammals, in addition to their known involvement in somatic growth, including the development of peripheral sexual organs[6,7]. This infantile 'critical period', lasting just a few days, corresponds to the first centrally driven, gonad-independent activation of the HPG axis and resulting surge in gonadotropin levels. This phenomenon, known as mini-puberty in humans, is the first of three activational periods that primes the HPG axis for puberty and adult fertility, setting in motion, for example, the growth of the first wave of ovarian follicles that will ovulate at puberty in females and the development of the testes in males (see ref. 15 for review). We show that during this critical period a switch in miRNA expression in turn flips a switch in a multilayered array of GnRH gene activators and repressors, permitting the sustained increase of the neurohormone required for subsequent sexual maturation. Two miRNA species act as the linchpins of this process: the miR-200/429 family, which is not only upregulated during this critical period but selectively enhanced in GnRH neurons, and miR-155, which appears to act on other hypothalamic cell types as well, and mediates, for example, the effects of a concomitant release of NO upstream of GnRH neurons. Interfering with the binding and function of these two key species blunts the infantile increase in *GnRH* expression, and the *in vivo* alteration of the miR-200/429–transcription factor micronetwork leads to the disruption of normal puberty onset as well as normal estrous cyclicity in adulthood.

The fact that GnRH neurons form an extremely small population (~800 neurons in a mouse brain) and their scattered distribution in a continuum from the olfactory bulb to the hypothalamus, albeit with a strong concentration in the hypothalamic preoptic area, have made genetic and epigenetic studies in these neurons a technical challenge until now. Our successful separation of GnRH from non-GnRH cells in the preoptic region of *GnRH::Gfp* mice has allowed us to determine miRNA expression profiles specific to this limited population of neurons in the postnatal brain (i.e., once differentiation and the establishment of connectivity, including their projection over several millimeters to the hypothalamic median eminence, are complete). The difficulty of this approach is evident from the fact that other such studies, even those focusing on more abundant neuronal types, have not always succeeded[40]. Using this approach we were not only able to study changes in miRNA expression in GnRH neurons at different stages of development, but to analyze the effects of the selective invalidation of miRNA biogenesis and acute manipulation of specific miRNA networks on the expression of transcription factors, *Gnrh* promoter activity and GnRH expression in the postnatal brain *in vivo*.

We demonstrated the specific role of miRNAs in sustaining postnatal GnRH expression by generating *Gnrh::cre;Dicer*$^{loxP/loxP}$ mice, in which Cre-mediated *Dicer* excision should have occurred as soon as the *Gnrh* promoter was first activated during embryonic development, at E14.5 (ref. 41), early enough for any miRNA effects on GnRH neuronal migration or integration into hypothalamic circuits to be apparent. Our findings show that miRNA processing in GnRH neurons is required for sexual development but not GnRH neuronal migration *in vivo*; the latter observation is in contrast with the reported involvement of miRNAs in the migration of other brain neuronal populations[42]. Indeed, GnRH expression appears normal during the perinatal and early infantile periods, and the process of sexual maturation commences normally and leads to vaginal opening in 70% of our mice. However, these mice never achieve puberty because of the progressive decline in *Gnrh* promoter activity from the second week of postnatal life (P7 to P12) and its complete extinction during the juvenile period. Our data indicate that miRNA species whose expression is upregulated in GnRH neurons during this critical period include miR-155 and members of the miR-200 family. Notably, the 100-fold enrichment of miR-200 family members is

restricted to GnRH neurons, indicating a highly specific function for these miRNA species in the regulation of infantile GnRH expression. We have identified several genes targeted directly or indirectly by miR-155 and miR-200/429, whose repression (for example, *Cebpb* and *Zeb1*) or activation (for example, *Pou2f1* and *Meis1*, which are both targets for Zeb1) are required for normal GnRH expression at P12, corresponding to the first centrally driven activation of the HPG axis and resulting gonadotropin surge in mice (**Supplementary Fig. 13**). In particular, the miR-200/429 family and its target Zeb1, which can directly repress the *Gnrh* promoter, also seem to form a double-negative loop with the key *Gnrh* promoter activator Pou2f1, while miR-155 counteracts NO/Cebpb-dependent GnRH repression. Nor can we rule out the possibility that some promoter modulators act as both activators and repressors depending on physiological conditions and cellular context, or exert a reciprocal regulatory effect on the miRNAs that control their expression. For instance, Cebpb, a *Gnrh* promoter repressor, nevertheless increases Zeb1 levels in GnRH neurons but not in non-GnRH hypothalamic cells (which do not express miR-200/429), while Zeb1 is known to provide negative feedback to miR-200/429 (ref. 19).

The expression patterns of various known *Gnrh* promoter modulators at P12 are not the same. While activators that are upregulated specifically in GnRH neurons in wild-type mice at P12 show reduced expression with the blockade of miR-200/429 binding (with the exception of Dlx5, whose transcript has no Zeb1 binding site and is thus probably regulated by other miRNA-effector pathways), the expression of one known activator, Dlx1 (ref. 43), is increased. Apart from a possible indirect effect, Dlx1 expression shows a downward trend in wild-type GnRH neurons at P12, unlike Pou2f1 or Meis1, which could explain this seeming paradox. The lack of effect of a miRNA-200/429 blockade on the expression of GnRH activator genes that contain no or few Zeb1-binding sites and that are not differentially expressed during the infantile–juvenile transition in GnRH neurons (but that could nevertheless influence baseline GnRH production or its regulation in other physiological contexts) further highlights the importance of the miR-200/Zeb1/Cebpb switch in the prepubertal increase in GnRH expression.

Both miR-155 (by interfering with NO/Cebpb-mediated signaling by nNOS neurons, themselves activated by kisspeptin[32]) and miR-200/429 (through Zeb1) could also influence GnRH expression by modulating the intricate relationship between different cells of the hypothalamic GnRH network through their effect on the expression of the kisspeptin receptor Gpr54, and thus on kisspeptin-Gpr54–mediated activation of GnRH expression (**Supplementary Fig. 13**). Kisspeptidergic fibers arising from the arcuate nucleus of the hypothalamus (ARH), like the axons of all ARH neurons, first reach the preoptic region around P12 and only achieve their final distribution by the end of the infantile period in both males and females[34,35]. The subsequent formation of new synaptic contacts with GnRH cell bodies and dendritic pruning[44] could be among the triggers of the miRNA-mediated switch in the control of *Gnrh* promoter activity during this period (**Supplementary Fig. 13**). NO itself, through its involvement in synapse formation, elimination and efficacy[45,46], and later through its essential function in puberty initiation[33] and its participation in the repression of GnRH expression[17], could play a more complex role than suspected heretofore. The kisspeptin–nNOS–GnRH neuronal microcircuit and miRNA–gene network in GnRH neurons (**Supplementary Fig. 13**) would thus be ideally positioned to ignite rhythmic GnRH gene transcription and pulsatile GnRH secretion[47] at puberty in response to developmental and bodily cues during the infantile period[15].

There might also be other microcircuits and feedback loops, possibly involving the expression of miR-155 in other cell types, as suggested by the fact that simultaneously neutralizing both miR-200/429–Zeb1 binding and miR-155–Cebpb binding resulted in a considerably weaker effect on peripubertal LH levels than miR-200/429 blockade alone. While blocking miR-200/429–Zeb1 binding during this infantile-juvenile critical period suppressed *Gnrh* promoter activity at the cellular level, these animals went on to display precocious, not delayed, puberty. Our data suggest that this counter-intuitive finding could in fact stem from a rebound effect, whereby the prolonged inhibition of GnRH expression (TSBs, once injected, remain at the injection site for around 2 weeks) results in a compensatory spike once the inhibition is relieved (**Supplementary Fig. 12b**). Such a phenomenon has been demonstrated previously in humans: children whose GnRH system is blunted by exposure to endocrine disruptors of agricultural origin undergo precocious puberty when they migrate to countries that do not use them[48].

While our study was primarily performed in mice, miRNA expression profiles available from RNAseq repositories for human tissues (for example, http://www.gtexportal.org/home/) indicate that miR155 is also widely distributed in the hypothalamus and other brain regions in humans. In contrast, the expression of miR-200 family members is, as described in mice[6], below the limit of detection in human brain tissues including the hypothalamus, an observation consistent with the restriction of these miRNA species to the sparse GnRH neuronal population. The Allen Human Brain Atlas (http://human.brain-map.org/) also shows the coexpression of *ZEB1* and *CEBPB* with *GNRH1* in regions of the diencephalon overlapping the hypothalamus (**Supplementary Fig. 14**). Taken together, these *in silico* data, combined with our ChIP assays identifying ZEB1 binding sites in the human *GNRH1* promoter (**Supplementary Fig. 8c**), suggest that the miRNA-*Gnrh* promoter modulator network identified in this study (**Supplementary Fig. 13**) may also be physiologically relevant for HPG axis activation during mini-puberty and continued sexual maturation in humans[49].

To conclude, our data indicate not only that miRNAs are active in the hypothalamic GnRH network, but that miRNA-200/429 and miRNA-155 are key components of a complex developmental switch that controls *Gnrh* promoter activity (**Supplementary Fig. 13**), whose correct functioning is essential for the normal initiation of puberty and adult fertility. Moreover, this switch in gene expression appears to involve a multilayered and interconnected array of miRNAs and their target genes in GnRH neurons, with its own built-in feedback control mechanism that alters the balance between inductive and repressive signals during the infantile critical period and thus leads to increased GnRH production. Deciphering the mechanisms through which miRNAs contribute to precocious or delayed puberty through their actions on GnRH neural network function may thus not only provide insights into the epigenetic regulation of maturational processes, but may also pave the way to a better understanding of idiopathic infertility[50] and the elaboration of new diagnostic and therapeutic options in humans.

METHODS

Methods and any associated references are available in the online version of the paper.

Note: Any Supplementary Information and Source Data files are available in the online version of the paper.

ACKNOWLEDGMENTS

A.M. was a postdoctoral fellow supported by the Fondation pour la Recherche Médicale (FRM). We are indebted to D. Accili for his help in conducting the

ChIP assays. We thank M. Tardivel (microscopy core facility), M.-H. Gevaert (histology core facility), D. Taillieu and J. Devassine (animal core facility) and the BICeL core facility of the Lille University School of Medicine for expert technical assistance. This research was supported by the FRM (Equipe FRM 2005 and DEQ20130326524, France to V.P.), grant BFI2011-025021 from the Spanish Ministry of Economy and Science (M.T.-S.), the ERC COST action BM1015 (V.P., P.G. and M.T.-S.) and the Fondation Bettencourt Schueller (F.L.).

AUTHOR CONTRIBUTIONS

A.M., F.L., K.C., J.R., S.R., F.G., M.T.-S., P.G. and V.P. designed the experiments. A.M., F.L., K.C., J.R., N.J., S.G., F.G., J.P., P.G. and V.P. performed the experiments. A.M. and V.P. analyzed the data. All authors discussed the results and A.M., J.R., S.R., M.T.-S., P.G. and V.P. wrote the manuscript.

COMPETING FINANCIAL INTERESTS

The authors declare no competing financial interests.

1. Ojeda, S.R. & Lomniczi, A. Puberty in 2013: unraveling the mystery of puberty. *Nat. Rev. Endocrinol.* **10**, 67–69 (2014).
2. Schwanzel-Fukuda, M., Bick, D. & Pfaff, D.W. Luteinizing hormone-releasing hormone (LHRH)-expressing cells do not migrate normally in an inherited hypogonadal (Kallmann) syndrome. *Brain Res. Mol. Brain Res.* **6**, 311–326 (1989).
3. Mason, A.J. *et al.* A deletion truncating the gonadotropin-releasing hormone gene is responsible for hypogonadism in the HPG mouse. *Science* **234**, 1366–1371 (1986).
4. de Roux, N. *et al.* A family with hypogonadotropic hypogonadism and mutations in the gonadotropin-releasing hormone receptor. *N. Engl. J. Med.* **337**, 1597–1602 (1997).
5. Harfe, B.D., McManus, M.T., Mansfield, J.H., Hornstein, E. & Tabin, C.J. The RNaseIII enzyme Dicer is required for morphogenesis but not patterning of the vertebrate limb. *Proc. Natl. Acad. Sci. USA* **102**, 10898–10903 (2005).
6. Hasuwa, H., Ueda, J., Ikawa, M. & Okabe, M. miR-200b and miR-429 function in mouse ovulation and are essential for female fertility. *Science* **341**, 71–73 (2013).
7. Papaioannou, M.D. & Nef, S. microRNAs in the testis: building up male fertility. *J. Androl.* **31**, 26–33 (2010).
8. Bernstein, E., Caudy, A.A., Hammond, S.M. & Hannon, G.J. Role for a bidentate ribonuclease in the initiation step of RNA interference. *Nature* **409**, 363–366 (2001).
9. Yoon, H., Enquist, L.W. & Dulac, C. Olfactory inputs to hypothalamic neurons controlling reproduction and fertility. *Cell* **123**, 669–682 (2005).
10. d'Anglemont de Tassigny, X., Ackroyd, K.J., Chatzidaki, E.E. & Colledge, W.H. Kisspeptin signaling is required for peripheral but not central stimulation of gonadotropin-releasing hormone neurons by NMDA. *J. Neurosci.* **30**, 8581–8590 (2010).
11. Urbanski, H.F. & Ojeda, S.R. A role for N-methyl-D-aspartate (NMDA) receptors in the control of LH secretion and initiation of female puberty. *Endocrinology* **126**, 1774–1776 (1990).
12. Wierman, M.E., Kiseljak-Vassiliades, K. & Tobet, S. Gonadotropin-releasing hormone (GnRH) neuron migration: initiation, maintenance and cessation as critical steps to ensure normal reproductive function. *Front. Neuroendocrinol.* **32**, 43–52 (2011).
13. Forni, P.E. & Wray, S. GnRH, anosmia and hypogonadotropic hypogonadism--where are we? *Front. Neuroendocrinol.* **36**, 165–177 (2015).
14. Prevot, V. *et al.* Normal female sexual development requires neuregulin-erbB receptor signaling in hypothalamic astrocytes. *J. Neurosci.* **23**, 230–239 (2003).
15. Prevot, V. Puberty in mice and rats. in *Knobil and Neill's Physiology of Reproduction* (eds. Plant, T.M. & Zeleznik, J.) 1395–1439 (Elsevier, New York, 2015).
16. Kuiri-Hänninen, T., Sankilampi, U. & Dunkel, L. Activation of the hypothalamic-pituitary-gonadal axis in infancy: minipuberty. *Horm. Res. Paediatr.* **82**, 73–80 (2014).
17. Belsham, D.D. & Mellon, P.L. Transcription factors Oct-1 and C/EBPbeta (CCAAT/enhancer-binding protein-beta) are involved in the glutamate/nitric oxide/cyclic-guanosine 5′-monophosphate-mediated repression of mediated repression of gonadotropin-releasing hormone gene expression. *Mol. Endocrinol.* **14**, 212–228 (2000).
18. Lee, V.H., Lee, L.T. & Chow, B.K. Gonadotropin-releasing hormone: regulation of the GnRH gene. *FEBS J.* **275**, 5458–5478 (2008).
19. Burk, U. *et al.* A reciprocal repression between ZEB1 and members of the miR-200 family promotes EMT and invasion in cancer cells. *EMBO Rep.* **9**, 582–589 (2008).
20. Le Béchec, A. *et al.* MIR@NT@N: a framework integrating transcription factors, microRNAs and their targets to identify sub-network motifs in a meta-regulation network model. *BMC Bioinformatics* **12**, 67 (2011).
21. van Rooij, E., Purcell, A.L. & Levin, A.A. Developing microRNA therapeutics. *Circ. Res.* **110**, 496–507 (2012).
22. Alisi, A. *et al.* Mirnome analysis reveals novel molecular determinants in the pathogenesis of diet-induced nonalcoholic fatty liver disease. *Lab. Invest.* **91**, 283–293 (2011).
23. Klein, D. *et al.* MicroRNA expression in alpha and beta cells of human pancreatic islets. *PLoS One* **8**, e55064 (2013).
24. Dweep, H., Sticht, C., Pandey, P. & Gretz, N. miRWalk--database: prediction of possible miRNA binding sites by "walking" the genes of three genomes. *J. Biomed. Inform.* **44**, 839–847 (2011).
25. Costinean, S. *et al.* Src homology 2 domain-containing inositol-5-phosphatase and CCAAT enhancer-binding protein beta are targeted by miR-155 in B cells of Emicro-MiR-155 transgenic mice. *Blood* **114**, 1374–1382 (2009).
26. Koch, M., Mollenkopf, H.J., Klemm, U. & Meyer, T.F. Induction of microRNA-155 is TLR- and type IV secretion system-dependent in macrophages and inhibits DNA-damage induced apoptosis. *Proc. Natl. Acad. Sci. USA* **109**, E1153–E1162 (2012).
27. Rodriguez, A. *et al.* Requirement of bic/microRNA-155 for normal immune function. *Science* **316**, 608–611 (2007).
28. Yang, J.H., Li, J.H., Jiang, S., Zhou, H. & Qu, L.H. ChIPBase: a database for decoding the transcriptional regulation of long non-coding RNA and microRNA genes from ChIP-Seq data. *Nucleic Acids Res.* **41**, D177–D187 (2013).
29. Heinz, S. *et al.* Simple combinations of lineage-determining transcription factors prime cis-regulatory elements required for macrophage and B cell identities. *Mol. Cell* **38**, 576–589 (2010).
30. Lefterova, M.I. *et al.* Cell-specific determinants of peroxisome proliferator-activated receptor gamma function in adipocytes and macrophages. *Mol. Cell. Biol.* **30**, 2078–2089 (2010).
31. Novaira, H.J., Fadoju, D., Diaczok, D. & Radovick, S. Genetic mechanisms mediating kisspeptin regulation of GnRH gene expression. *J. Neurosci.* **32**, 17391–17400 (2012).
32. Hanchate, N.K. *et al.* Kisspeptin-GPR54 signaling in mouse NO-synthesizing neurons participates in the hypothalamic control of ovulation. *J. Neurosci.* **32**, 932–945 (2012).
33. Bellefontaine, N. *et al.* Leptin-dependent neuronal NO signaling in the preoptic hypothalamus facilitates reproduction. *J. Clin. Invest.* **124**, 2550–2559 (2014).
34. Rameau, G.A. *et al.* Biphasic coupling of neuronal nitric oxide synthase phosphorylation to the NMDA receptor regulates AMPA receptor trafficking and neuronal cell death. *J. Neurosci.* **27**, 3445–3455 (2007).
35. Bouret, S.G., Draper, S.J. & Simerly, R.B. Formation of projection pathways from the arcuate nucleus of the hypothalamus to hypothalamic regions implicated in the neural control of feeding behavior in mice. *J. Neurosci.* **24**, 2797–2805 (2004).
36. Caron, E., Ciofi, P., Prevot, V. & Bouret, S.G. Alteration in neonatal nutrition causes perturbations in hypothalamic neural circuits controlling reproductive function. *J. Neurosci.* **32**, 11486–11494 (2012).
37. Grueter, C.E. *et al.* A cardiac microRNA governs systemic energy homeostasis by regulation of MED13. *Cell* **149**, 671–683 (2012).
38. Lomniczi, A. *et al.* Epigenetic control of female puberty. *Nat. Neurosci.* **16**, 281–289 (2013).
39. Lomniczi, A. *et al.* Epigenetic regulation of puberty via Zinc finger protein-mediated transcriptional repression. *Nat. Commun.* **6** http://dx.doi.org/10.1038/ncomms10195 (2015).
40. Issler, O. *et al.* MicroRNA 135 is essential for chronic stress resiliency, antidepressant efficacy, and intact serotonergic activity. *Neuron* **83**, 344–360 (2014).
41. Hanchate, N.K. *et al.* SEMA3A, a gene involved in axonal pathfinding, is mutated in patients with Kallmann syndrome. *PLoS Genet.* **8**, e1002896 (2012).
42. Franzoni, E. *et al.* miR-128 regulates neuronal migration, outgrowth and intrinsic excitability via the intellectual disability gene *Phf6*. *eLife* **4** http://dx.doi.org/10.7554/eLife.04263 (2015).
43. Givens, M.L. *et al.* Developmental regulation of gonadotropin-releasing hormone gene expression by the MSX and DLX homeodomain protein families. *J. Biol. Chem.* **280**, 19156–19165 (2005).
44. Cottrell, E.C., Campbell, R.E., Han, S.K. & Herbison, A.E. Postnatal remodeling of dendritic structure and spine density in gonadotropin-releasing hormone neurons. *Endocrinology* **147**, 3652–3661 (2006).
45. Garthwaite, J. From synaptically localized to volume transmission by nitric oxide. *J. Physiol. (Lond.)* **594**, 9–18 (2016).
46. Cossenza, M. *et al.* Nitric oxide in the nervous system: biochemical, developmental, and neurobiological aspects. *Vitam. Horm.* **96**, 79–125 (2014).
47. Choe, H.K. *et al.* Real-time GnRH gene transcription in GnRH promoter-driven luciferase-expressing transgenic mice: effect of kisspeptin. *Neuroendocrinology* **102**, 194–199 (2015).
48. Parent, A.S. *et al.* The timing of normal puberty and the age limits of sexual precocity: variations around the world, secular trends, and changes after migration. *Endocr. Rev.* **24**, 668–693 (2003).
49. Chachlaki, K. & Prévot, V. Coexpression profiles reveal hidden gene networks. *Proc. Natl. Acad. Sci. USA* **113**, 2563–2565 (2016).
50. Boehm, U. *et al.* Expert consensus document: European Consensus Statement on congenital hypogonadotropic hypogonadism—pathogenesis, diagnosis and treatment. *Nat. Rev. Endocrinol.* **11**, 547–564 (2015).

ONLINE METHODS

Animals. All mice were group-housed under specific pathogen-free conditions in a temperature-controlled room (21–22 °C) with a 12-h light–dark cycle and *ad libitum* access to food and water. C57Bl/6J *Gnrh::cre*(Tg(*Gnrh1::cre*)1Dlc), C57Bl/6J *Dicer*$^{LoxP/LoxP}$, and C57Bl/6J *Gnrh::Gfp* mice were a generous gift of Dr. Catherine Dulac (Howard Hughes Medical Institute, Cambridge MA)[9], Dr. Brian Harfe (University of Florida, FL)[5] and Dr. Daniel J. Spergel (Section of Endocrinology, Department of Medicine, University of Chicago, IL)[51], respectively. *tdTomato*$^{loxP/STOP}$ mice (B6.Cg-*Gt(ROSA)26Sortm9(CAG-tdTomato)Hze*/J) were purchased from the Jackson laboratory (Maine, USA). Mice were genotyped by PCR using primers listed in **Supplementary Table 3**. Animal studies were approved by the Institutional Ethics Committees for the Care and Use of Experimental Animals of the Universities of Lille and Cordoba; all experiments were performed in accordance with the guidelines for animal use specified by the European Union Council Directive of September 22, 2010 (2010/63/EU). The sex of the animals used in specified in the text and/or figure legends, except for experiments assessing GnRH neuronal migration, postnatal GnRH expression and real time-PCR analyses on FACS-sorted GnRH neurons, in which animals of both sexes were used. Investigators were blind to the genotype or treatment group of animals except when morphological or physiological differences were too obvious to be ignored. Heterozygous *Gnrh::cre;Dicer*$^{LoxP/+}$ littermates were excluded from the analyses.

Physiological measurements. *Fertility index.* Male and female fertility indices were calculated from the number of litters per females during a 120-d mating.

Puberty onset. Weaned female mice were checked daily for vaginal opening. After vaginal opening, vaginal smears were performed daily and analyzed under an inverted microscope to identify the specific day of the estrous cycle. Weaned males were checked daily for balanopreputial separation.

Hormone level measurements. Protocols and doses for *in vivo* testing of the LH response to GnRH, kisspeptin-10 and NMDA were as described in detail elsewhere[52]. Serum LH and FSH levels were measured using radioimmunoassay kits supplied by the National Institutes of Health (Dr. A.F. Parlow, National Hormone and Peptide Program, Torrance, CA). Rat LH-I-10 and FSH-I-9 were labeled with ^{125}I using Iodo-gen tubes, following the instructions of the manufacturer (Pierce, Rockford, IL). Hormone concentrations were determined using reference preparations of LH-RP-3 and FSH-RP-2 as standards. Intra- and inter-assay coefficients of variation were <8 and 10% for LH and <6 and 9% for FSH, respectively. The sensitivity of the assay was 3.75 pg/tube for LH and 20 pg/tube for FSH. The accuracy of hormone measurements was confirmed by the assessment of rodent serum samples of known concentration (external controls).

Pharmacological inhibition of NOS activity. *N*-G-nitro-L-arginine methyl ester, HCl (L-NAME; N5751, Sigma) was used to inhibit the activity of nitric oxide synthase in infantile mice. *Gnrh::Gfp;Gnrh::cre;Dicer*$^{LoxP/LoxP}$ mice received a single intraperitoneal injection of L-NAME (50 mg/kg, i.p.) or vehicle (saline) on P11 and were killed 12 h later for GnRH neuron isolation by FACS.

Gonadal histology and quantitative analysis. Ovaries and testes were collected from 3-month-old *Dicer*$^{LoxP/LoxP}$ and *Gnrh::cre;Dicer*$^{LoxP/LoxP}$ mice, immersion-fixed in 4% PFA solution and stored at 4 °C. Paraffin-embedded ovaries and testes were sectioned at a thickness of 5 µm (histology facility, University of Lille 2, France) and stained with hematoxylin-eosin.

Tissue preparation. For immunohistochemical analysis, embryos were obtained after cervical dislocation from timed-pregnant *Gnrh::cre;Dicer*$^{LoxP/+}$ crossed with *Gnrh::cre;Dicer*$^{LoxP/LoxP}$ male mice. Embryos were washed thoroughly in cold 0.1 M PBS, fixed in fixative solution (4% paraformaldehyde (PFA), 0.2% picric acid in 0.1 M PBS, pH 7.4) for 6–8 h at 4 °C and cryoprotected in 20% sucrose overnight at 4 °C. The following day, embryos were embedded in OCT embedding medium (Tissue-Tek), frozen on dry ice, and stored at −80 °C until sectioning. Postnatal (P0 to P28) and adult mice (3–5 months old) were anesthetized with 50–100 mg/kg of ketamine-HCl and 5–10 mg/kg xylazine-HCl and perfused transcardially with 2–10 ml of saline, followed by 10–100 ml of 4% PFA, pH 7.4. Brains were collected, postfixed in the same fixative for 2 h at 4 °C, embedded in OCT embedding medium (Tissue-Tek), frozen on dry ice, and stored at −80 °C until cryosectioning.

Immunohistochemistry and GnRH neuron quantification. Tissues were cryosectioned (Leica cryostat) at 16 µm for embryos and pre-weaning postnatal mice, and at 35 µm (free-floating sections) for post-weaning and adult brains. Immunohistochemistry was performed as previously reported[53,54], using Alexa-Fluor 488- (1:400) and Cy3-conjugated (1:800) secondary antibodies (Invitrogen, A11008). Fluorescent specimens were mounted using 1,4-diazabicyclo[2.2.2]octane (Sigma-Aldrich). The primary antisera used were as follows: rabbit anti-GnRH (1:3000), a generous gift from Prof. G. Tramu (Centre Nationale de la Recherche Scientifique, URA 339, Université Bordeaux I, Talence, France)[55]. As the GnRH neuronal population is very limited in the mouse brain (about 800 neurons), all neurons were counted by eye under the microscope in two out of three series of brain (adult) or head (embryos and P0) sections encompassing the entire nasal and/or forebrain regions, as reported previously[53].

Digital image acquisition. Sections were analyzed using an Axio Imager.Z1 ApoTome microscope (Zeiss, Germany), equipped with a motorized stage and an AxioCam MRm camera (Zeiss, Germany). Specific filter cubes were used for the visualization of green (EX: 475/40 nm, DM: 500 nm, BA: 530/50 nm), red (EX: 550/25 nm, DM: 570 nm, BA: 605/70 nm), and UV (bisbenzimide) or AMCA (amino-methyl-coumarin-acetate) fluorescence (EX: 365 nm, DM: 395 nm, BA: 445/50 nm).

To create photomontages, single-plane images were captured sequentially for each fluorophore using the MosaiX module of the AxioVision 4.6 system (Zeiss, Germany) and a Zeiss 20× objective (N.A. 0.8). High magnification photomicrographs represent maximal intensity projections derived from a series of triple-ApoTome adjacent images collected at 0.310 µm intervals using the z-stack module of the AxioVision 4.6 system and a Zeiss 40× oil immersion objective (N.A. 1.3). All images were captured in a stepwise fashion over a defined z-focus range corresponding to all visible staining within the section and consistent with the optimum step size for the corresponding objective and the wavelength (λ = 500 nm). Adobe Photoshop (Adobe Systems, San Jose, CA) was then used to process the images, adjust brightness and contrast, and merge them.

Isolation of hypothalamic GnRH neurons using fluorescence-activated cell sorting. The preoptic regions of *Gnrh::Gfp;Dicer*$^{LoxP/LoxP}$ and *Gnrh::Gfp;Gnrh::cre;Dicer*$^{LoxP/LoxP}$ mice were microdissected and enzymatically dissociated using a Papain Dissociation System (Worthington, Lakewood, NJ) to obtain single-cell suspensions. FACS was performed using an EPICS ALTRA Cell Sorter Cytometer device (BD Bioscience). The sort decision was based on measurements of GFP fluorescence (excitation: 488 nm, 50 mW; detection: GFP bandpass 530/30 nm, autofluorescence bandpass 695/40 nm) by comparing cell suspensions from *Gnrh::Gfp* and wild-type animals, as indicated in **Supplementary Figure 7**. For each animal, 400 to 800 GFP-positive cells were sorted directly into 10 µl of extraction buffer: 0.1% Triton® X-100 (Sigma-Aldrich) and 0.4 unit/µl RNaseOUT™ (Life Technologies).

Quantitative RT-PCR analyses. For gene expression analyses, mRNAs obtained from FACS-sorted GnRH neurons were reverse transcribed using SuperScript® III Reverse Transcriptase (Life Technologies) and a linear preamplification step was performed using the TaqMan® PreAmp Master Mix Kit protocol (P/N 4366128, Applied Biosystems). Real-time PCR was carried out on Applied Biosystems 7900HT Fast Real-Time PCR System using exon-boundary-specific TaqMan® Gene Expression Assays (Applied Biosystems): *Aes* (Aes-Mm00507847_m1), *Cebpb* (Cebpb-Mm00843434_s1), *Dicer* (Mm00521722_m1), *Dlx1*(Dlx1-Mm00438424_m1), *Dlx5* (Dlx5-Mm00438430_m1), *Gfp* (Gfp-Mr03989638_mr), *Gnrh1* (Gnrh1-Mm01315605_m1), *Gpr54* (*Gpr54*-Mm00475046_m1), *Lpin1* (Lpin1-Mm00550511_m1), *Maf* (Maf-Mm02581355_s1), *Meis1* (Meis1-Mm00487664_m1), *Msx1* (Msx1-Mm00440330_m1), *Otx2* (Otx2-Mm00446859_m1), *Pbx1* (Pbx1-Mm04207617_m1), *Pknox1* (Pknox1-Mm00479320_m1), *Pou2f1* (Pou2f1-Mm00448332_m1), *Tle4* (Tle4-Mm01195172_m1) and *Zeb1* (Zeb1-Mm00495564_m1). Control housekeeping genes: *r18S* (18S-Hs99999901_s1) and ACTB (Actb-Mm00607939_s1).

MicroRNA expression analyses were performed using stem-loop RT-PCR based TaqMan Rodent MicroRNA Arrays (Applied Biosystems). Briefly, miRNAs obtained from FACS-sorted GnRH neurons were reverse transcribed using the TaqMan miRNA Reverse Transcription Kit (Applied Biosystems) in combination with the stem-loop Megaplex primer pool sets A and B according to

the manufacturer's instructions. A linear preamplification step was performed using the TaqMan® PreAmp Master Mix Kit protocol (P/N 4366128, Applied Biosystems) and quantitative real-time PCR were performed using TaqMan Low-Density Arrays (Applied Biosystems) on an Applied Biosystems 7900HT thermocycler using the manufacturer's recommended cycling conditions.

Gene and miRNA expression data were analyzed using SDS 2.4.1 and Data Assist 3.0.1 software (Applied Biosystems), with R18S and actin as control housekeeping mRNAs and U6sRNA as control housekeeping miRNA following a standardized procedure[56]. Assay-centric heat-maps were generated with Data Assist 3.0.1 by unsupervised hierarchical clustering (complete linkage) using Pearson's correlation as a distance measure.

Zeb1 chromatin immunoprecipitation (ChIP) assays. Immortalized GnRH neurons (GN11 cells) were cultured in DMEM + 10% FBS (Life Technology). Prior to experimental assays, cells were washed twice in PBS and incubated overnight in serum-free medium. The next morning, 10% FBS was added for 2 h. Chromatin isolation was performed using the ChIP-IT Express kit (Active Motif) following the manufacturer's instructions. After DNA shearing by sonication (9 min total, 20-s pulses at 70% power followed by a 40-s pause; on ice), protein-bound DNA was immunoprecipitated at 4 °C overnight using 5 µg of a polyclonal goat anti-rabbit Zeb1 antibody (E20; Santa Cruz Biotechnology; SC-10572) or control goat IgG (Santa Cruz Biotechnology; sc-2028). ChIP-DNA fragments were purified using a QIAquick PCR purification kit (Qiagen), and analyzed by qPCR on a CFX96 thermal cycler (Bio-Rad) using GoTaq® qPCR Master Mix (Promega) and the primers indicated in **Supplementary Table 4**.

Western blot analyses. The preoptic area of the hypothalamus was dissected from each animal using Wecker scissors (Moria, France) under a binocular magnifying glass, and protein extracted in 200 µl of lysis buffer (25 mM Tris, pH 7.4, β-glycerophosphate, 1.5 mM EGTA, 0.5 mM EDTA, 1 mM sodium pyrophosphate, 1 mM sodium orthovanadate, 10 µg/ml leupeptin and pepstatin A, 10 µg/ml apoprotinin, 100 µg/ml PMSF and 1% Triton-X100) by trituration of the fragments through 22 and 26 gauge needles in succession. Tissue lysates were cleared by centrifugation at 14,000 rpm for 15 min at 4 °C. Protein content was determined using the sample buffer (Invitrogen). Samples were boiled for 5 min and stored at −80 °C until use. Samples were reboiled for 5 min after thawing and electrophoresed for 75 min at 150 V in 7% Tris-acetate, or for 50 min at 200 V in precast 4–12% MES SDS-polyacrylamide gels according to the protocol supplied with the NuPAGE system (Invitrogen). After size fractionation, the proteins were transferred onto 0.2 µm pore-size polyvinylidene difluoride membranes (LC2002; Invitrogen) in the blot module of the NuPAGE system (Invitrogen) for 75 min at room temperature. Membranes were blocked for 1 h in blocking buffer (TBS with 0.05% Tween 20 (TBST) and 5% nonfat milk) at room temperature, and incubated overnight at 4 °C with the appropriate primary antibody diluted in blocking buffer (rabbit polyclonal anti-RFP, 600-401-379, 1:1,000, Rockland Antibodies & Assays; rabbit polyclonal anti-nNOS, sc-8309, 1:500, Santa Cruz technologies; rabbit polyclonal anti-Ser1412 phospho-nNOS, PA1-032; 1:1,000, Affinity BioReagents; goat polyclonal anti-actin, sc-1616, 1:1,000). Membranes were washed four times with TBST the following day before being exposed to HRP-conjugated secondary antibodies (Vector, peroxidase-labeled anti rabbit and anti goat IgGs PI-1000 and PI9500, respectively) diluted in blocking buffer for 1 h at room temperature. Immunoreactions were visualized using the ECL detection kit (NEL101; PerkinElmer, Boston, MA). Immunoblots were scanned using a desktop scanner (Epson Expression 1680 PRO) and Adobe Photoshop, and band intensities were determined using ImageJ software (NIH, Bethesda).

Target site blockers (TSBs). To selectively hamper the *in vivo* silencing activity of miR-155 and miR-200b/200c/429 on *Cebpb* and *Zeb1*, respectively, we used custom-designed target site blockers with phosphorothioate backbone modifications from Exiqon (miRCURY LNA™ microRNA Target Site Blockers, *in vivo* ready). TSB sequences are designed with a large arm that covers the miRNA binding site and a short arm outside the miRNA seed to ensure target specificity. One sequence was generated to protect the unique miR-155-binding site in the *Cebpb* 3′ UTR (**Supplementary Fig. 9e**). Five sequences were generated to protect 200b/200c/429-binding sites in the *Zeb1* 3′ UTR (**Supplementary Fig. 8d**) and mixed at equimolar ratios (TSB-200).

Stereotactic brain infusions of TSBs. *Gnrh::Gfp* mice were placed in a stereotaxic frame (Kopf® Instruments, California) under anesthesia (isoflurane), and a burr hole was drilled 1 mm lateral to the bregma, according to a mouse brain atlas (Paxinos and Franklin, 2004). A 10 µl Hamilton syringe was slowly inserted into the bottom of the left lateral ventricle (3.5 mm deep relative to the dura), and 1 µl of the different treatment solutions (TSB-200, 50 µM; TSB-155, 50 µM) or vehicle (PBS, pH 7.4) was injected using an infusion pump (KD Scientific, Holliston, MA) over 4 min. Mice were randomly assigned to TSB injection. Animals were subjected to intracranial surgery at P9 and either killed at P12 or checked daily for puberty onset after weaning.

Identification of putative Zeb1-binding sites. To identify putative Zeb1 and C/EBPβ binding sites in the promoter regions of target genes, 1.5 Kb of the genomic sequence upstream of the transcription initiation site of GnRH, Gpr54 and the *Gnrh* promoter activators under study were analyzed using ALGEN PROMO 3.0 software (http://alggen.lsi.upc.es/cgi-bin/promo_v3/promo/promoinit.cgi?dirDB=TF_8.3) and JASPAR database (http://jaspar.genereg.net/).

Sample size and randomization statement. Sample sizes for physiological and neuroanatomical studies and for miRNA and gene expression analyses were estimated based on past experience and those presented in the literature. Typically, $n \geq 5$ mice from at least three different litters for each group were used to study sexual maturation and fertility; $n \geq 3$ mice from three different litters were collected to perform quantitative RT-PCR analyses in cells isolated by FACS; and $n \geq 3$ mice from three different litters each group were collected for anatomy and immunostaining. No randomization method was used to assign subjects in the experimental groups or to collect and process data.

Statistics. All analyses were performed using Prism 5 (GraphPad Software) and assessed for normality (Shapiro-Wilk test) and variance, when appropriate. Sample sizes were chosen according to standard practice in the field. Data were compared using an unpaired two-tailed Student's *t*-test, a one-way ANOVA for multiple comparisons or a two-way repeated measures ANOVA. A Mann-Whitney *U* test (non-parametric) was performed when appropriate. A non-parametric unpaired test (Mann-Whitney-Wilcoxon) was used to compare Western blot data. The significance level was set at $P < 0.05$. Data are indicated as means ± s.e.m. The number of biologically independent experiments, *P* values and degrees of freedom are indicated either in the main text or in the figure legends.

Data availability. The data that support the findings of this study are available from the corresponding author upon request.

A **Supplementary Methods Checklist** is available.

51. Spergel, D.J., Krüth, U., Hanley, D.F., Sprengel, R. & Seeburg, P.H. GABA- and glutamate-activated channels in green fluorescent protein-tagged gonadotropin-releasing hormone neurons in transgenic mice. *J. Neurosci.* **19**, 2037–2050 (1999).
52. García-Galiano, D. *et al.* Kisspeptin signaling is indispensable for neurokinin B, but not glutamate, stimulation of gonadotropin secretion in mice. *Endocrinology* **153**, 316–328 (2012).
53. Messina, A. *et al.* Dysregulation of Semaphorin7A/β1-integrin signaling leads to defective GnRH-1 cell migration, abnormal gonadal development and altered fertility. *Hum. Mol. Genet.* **20**, 4759–4774 (2011).
54. Giacobini, P. *et al.* Brain endothelial cells control fertility through ovarian-steroid-dependent release of semaphorin 3A. *PLoS Biol.* **12**, e1001808 (2014).
55. Beauvillain, J.C. & Tramu, G. Immunocytochemical demonstration of LH-RH, somatostatin, and ACTH-like peptide in osmium-postfixed, resin-embedded median eminence. *J.Histochem.Cytochem.* **28**, 1014–1017 (1980).
56. Schmittgen, T.D. & Livak, K.J. Analyzing real-time PCR data by the comparative C(T) method. *Nat. Protoc.* **3**, 1101–1108 (2008).

doi:10.1038/nn.4298

Corrigendum: A microRNA switch regulates the rise in hypothalamic GnRH production before puberty

Andrea Messina, Fanny Langlet, Konstantina Chachlaki, Juan Roa, Sowmyalakshmi Rasika, Nathalie Jouy, Sarah Gallet, Francisco Gaytan, Jyoti Parkash, Manuel Tena-Sempere, Paolo Giacobini & Vincent Prevot

***Nat. Neurosci.* 19, 835–844 (2016); published online 2 May 2016; corrected after print 3 June 2016**

In the version of this article initially published, the Figure 1e,f legend read, "Circulating levels of LH (left panels) and FSH (right panels) in GnRH cells of control (blue) and Dicer mutants (red)"; as the hormones were not measured in GhRH cells, it should have simply read "Circulating levels of LH (left panels) and FSH (right panels) in control (blue) and Dicer mutants (red)." Figure 2b was missing scale bars and has been replaced. The label "TSB-200" was missing from the rightmost bar in Figure 4d. And the treatment in Figure 5c was misidentified as TSB-200 instead of TSB-155. The errors have been corrected in the HTML and PDF versions of the article.